Supporting Information

A Fungal Nonribosomal Peptide Synthetase Module that can Synthesize Thiopyrazines

Kangjian Qiao[□], Hui Zhou[□], Wei Xu[□], Wenjun Zhang[□,□], Neil Garg[§], Yi Tang*[,□,§]

TABLE OF CONTENTS:

1. EXPERIMENTAL METHODS

1.1 Molecular Biology

Strains and General Techniques for DNA Manipulation

E. coli XL1-Blue and *E. coli* TOPO10 (Invitrogen) were used for cloning following standard recombinant DNA techniques. DNA restriction enzymes were used as recommended by the manufacturer (New England Biolabs). PCR was performed using Platinum *pfx* DNA polymerase (Invitrogen). The constructs of pCR-Blunt vector (Invitrogen) containing desired PCR products were confirmed by DNA sequencing. *E. coli* BL21(DE3) (Novagen) and BAP1 were used for protein expression.

Construction of C-terminus Hexahistidine Tagged NRPS325 Expression Plasmid

Genomic DNA from *A. terreus* was used as the template for PCR amplification. All the primers are listed in Table S2. The gene encoding NRPS325 (residues 2447-3890) was amplified with primer pair P1/P2, flanking the gene product with restriction sites *Nhe*I and *Not*I. The PCR product was first placed into a pCR-Blunt vector and sequenced to create pKJ74. Then, the gene product was prepared by digesting pKJ74 with *Nhe*I and *Not*I, and ligated into pET23a vector to generate NRPS325 expression plasmid pKJ75. The His193 to Ala and His194 to Ala mutations were introduced into pKJ75 by primer pairs P3/P4 and P5/P6 to give pKJ113 and pKJ114, respectively. The ATR tridomain and TR didomain genes were amplified using primer pairs P10/P12 and P11/P2. Then amplified genes were purified by agarose gel and digested with *NheI* and *NotI*. The digest products were directly ligated into pET23a vector to give ATR expression plasmid pKJ115 and pKJ116. Primer pair of P7 and P8 was used to introduce Gly1132Ala and Gly1135Ala into NRPS325 and the gene product was linked with P2/P9 gene product using

Splicing by Overlapping Extension (SOE) PCR. The resultant product was digested with *Spe*I and *Not*I and ligated into pKJ75 vector prepared using the same sites to yield NRPS325-G1132A-G1135A expression plasmid pKJ119.

1.2 Protein Expression and Purification

Expression and Purification of NRPS325 in *E. coli*.

The expression plasmid pKJ75 was transformed into *E. coli* BL21(DE3) strain and *E. coli* BAP1 strain for *apo*- and *holo*- protein expression, respectively. For 1 L of LB liquid culture, the cells were grown at 37 °C in LB medium with 100 μg/mL ampicillin to an OD_{600} of 0.4-0.6. At which time the cells were incubated on ice for 10 minutes, and then induced with 0.1 mM isopropyl thio-β-D-galactoside (IPTG) for 16 hours at 16°C. The cells were harvested by centrifugation (3500 rpm, 15 minutes, 4°C), re-suspended in 30 mL lysis buffer (50 mM Tris-HCl, 2 mM EDTA, 2 mM DTT, 500 mM NaCl, 5 mM imidazole, pH=7.9) and lysed using sonication on ice. Cellular debris was removed by centrifugation (30000 g, 30 min, 4°C). Ni-NTA agarose resin was added to the supernatant and the solution was stirred at 4°C for at least 2 hours. The protein resin mixture was loaded into a gravity flow column and proteins were purified with increasing concentration of imidazole in buffer A (50 mM Tris-HCl, 500 mM NaCl, pH=7.9). Purified NRPS325 were concentrated and buffered exchanged into buffer E (50 mM Tris-HCl, 100 mM NaCl, pH=7.9) + 10% glycerol. The final enzyme was concentrated, aliquoted and flash frozen. Protein yield was determined to be 25 mg/L, with the Bradford assay using BSA as a standard. NRPS325-H193A, NRPS325-H194A, ATR, TR and NRPS325-G1132A-G1135A were purified using the same protocol as described above and SDS page gels were shown in Figure S1.

1.3 In vitro Characterization of NRPS325

NRPS325 PPi Releasing Assays

Kinetic analysis of NRPS325 was performed using the Enzymatic Determination of Pyrophosphate Kit (Sigma-Aldrich), essentially following the manufacturer's protocol but with 100 μL assay volumes in a quartz 96-well microplate. In this assay, pyrophosphate (PPi) was hydrolyzed to inorganic phosphate (Pi) in the presence of D-fructose-6-phosphate (F-6-P) catalyzed by fructose-6-phosphate kinase (PPi-PFK). The byproduct D-fructose-1,6-phosphate (F-1,6-P) was further decomposed to D-glyceraldehyde-3-phosphate (GAP) and dihydroxyacetone phosphate (DHAP) catalyzed by aldolase. Under the control of Triosephosphate isomerase, GAP and DHAP can be transformed to each other. DHAP can be further reduced to glycerol-3-phosphate by glycerophosphate dehydrogenase (GDH) with the consumption of NADH (maximum absorption at 340nm). Therefore, the detection of PPi was indirectly connected to the consumption of NADH, which can be monitored spectrophotometrically at 340nm.[1]

Reactions (100 μL) contained 75 mM Tris-HCl (pH 7.5), 10 mM $MgCl_2$, 5 mM ATP, 0.25 mM NADH, 4 mM F-6-P, 0.2 units/mL PPi-PFK, 2.5 units/mL aldolase, 1.8 units/mL GDH and 20 units/mL TPI and 1 μM NRPS325 was used with 2 mM L-amino acid. Absorbance at 340 nm was measured over a 10-min interval in Biotek Microplate Spectrophotometer PowerWave XS. The spectrophotometer recorded data points every 20 s. Each assay was performed in duplicate. A linear reaction velocity was obtained by using a minimum of 20 co-linear data points and an extinction coefficient of 6400 $M^{-1}cm^{-1}$.

NRPS325 in vitro Turnover Assays

Reaction (50 µL) contained 10 µM NRPS325, 10 µM ApdA-PKS, 10 µM ApdC, 5 mM thiol, 10 mM amino acid, 20 mM ATP, 10 mM $MgCl_2$, 20 mM ATP and 2 mM NADPH in phosphate buffer was incubated at room temperature to produce thiopyrazines. All the in vitro assays were quenched after overnight reaction and extracted twice with an equal volume of ethyl acetate (EA). The organic phase was separated, evaporated to dryness, and re-dissolved in 20 µL of methanol. The organic residue was analyzed by LC-MS. LC-MS was conducted with a Shimadzu 2010 EV Liquid Chromatography Mass Spectrometer by using both positive and negative electrospray ionization and a Phenomenex Luna 5µ 2.0 x 100 mm C18 reverse-phase column. Samples were separated on a linear gradient of 5 to 95% CH_3CN (vol/vol) over 30 min and further 95% CH_3CN (vol/vol) for 20 min in H_2O supplemented with 0.05% (vol/vol) formic acid at a flow rate of 0.1mL/min at room temperature.

In vivo Large Scale Synthesis of Compound **2a** and NMR.

The pKJ75 encoding NRPS325 was transformed into *E. coli* BAP1 strain for production of compound **2a**. For 1 L liquid culture, the cells were grown at 37°C in TB medium with 100 µg/mL ampicillin to an OD_{600} of 0.4-0.6. 1 hour after induction, NAC was added to the final concentration 5 mM. Production level of **2a** was monitored by HPLC. After the product level had maximized (after 3 days), the reaction mixture was extracted three times with EA. The resultant organic extracts were combined and evaporated to dryness, re-dissolved in methanol and purified first by silica column, and followed by reverse-phase HPLC (XTerra Prep MS C18 5µm, 19 mm X 50 mm) on a linear gradient of 5 to 95% CH_3CN (v/v) over 15 min and 95% CH_3CN (v/v) further for 15 min in H_2O supplemented with 0.1% (v/v) trifluoroacetic acid at a flow rate of 2.5 mL/min. High resolution mass study of **2a** was performed VG ZAB2SE (1996)

high resolution mass spectrometer, with Opus V3.1 and DEC 3000 Alpha Station. 1D and 2D NMR of **2a** were performed on Bruker DRX-500 spectrometer using CD_3COCD_3 as the solvent.

Rate of **2a** Formation by NRPS325 and Variants.

The observed rate of **2a** formation was measured using 100 µL reaction mixtures containing 10 µM of NRPS325, 5 mM NAC, 10 mM L-Leucine, 10 mM $MgCl_2$, 20 mM ATP and 2 mM NADPH in phosphate buffer. Reactions were initiated by adding enzyme and incubated at room temperature 25°C. The reactions were quenched at 30 min, 1 hour, 2 hour, 3 hour and 4 hour respectively and analyzed by reverse-phase HPLC (Luna C18 5µm, 250 mm X 4.6 mm) on a linear gradient of 5 to 95% CH_3CN (v/v) over 30 min and 95% CH_3CN (v/v) further for 15 min in H_2O supplemented with 0.1% (v/v) trifluoroacetic acid at a flow rate of 1 mL/min. Production of **2a** was measured by integration of the peaks at 320 nm. Purified **2a** from in vivo system was used as a standard to quantify the production of **2a** in the in vitro assays.

NADPH Detection Assays.

Reaction mixture (100 µL) contains 10 µM of NRPS325, 5 mM NAC, 10 mM L-Leucine, 10 mM $MgCl_2$, 20 mM ATP and 2 mM NADPH in phosphate buffer. 2 mM NADPH dissolved in phosphate buffer was used as a control. Every 10 minutes, an aliquot of the reaction was diluted to 1:100 and absorbance at 340 nm was measured over a 10-min interval in Biotek Microplate Spectrophotometer PowerWave XS. Each reaction was repeated 3 times.

2. SUPPLEMENTARY TABLES AND FIGURES

2.1 Supplementary Table

Table S1. Sequences of primers used in the construction of plasmids.

No.	Primers	Sequences[a]
P1	NRPS325-f	5'- AA*GCTAGC***ATG**ACTCCACACACCGAAATCA-3'
P2	NRPS325-r	5'- AA*GCGGCCGC*CTGCCTCAATCCCTTA-3'
P3	H193A-f	5'- ATACCATTGTCTTCGGCTACgcTCATATCATCATGGATGGTG-3'
P4	H193A-r	5'- TATGGTAACAGAAGCCGATGcgAGTATAGTAGTACCTACCAC-3'
P5	H194-f	5'- ATACCATTGTCTTCGGCTACCATgcTATCATCATGGATGGTG-3'
P6	H194-r	5'- TATGGTAACAGAAGCCGATGGTAcgATAGTAGTACCTACCAC-3'
P7	G1132A-f	5'- ACACTAGTGGTTCCACTGGGAAGCCAAAGGGTATCA-3'
P8	G1132A1135A-r	5'- CTCACTGGCAGCACTGCGTTCCTGGGCCGTGCGATCGTTC-3'
P9	G1132A1135A-f2	5'- CCTGGGCCGTGCGATCGTTCGACAGCTTAT-3'
P10	ATR-f	5'- AA*GCTAGC***ATG**GATGAGTCTTTGGTCAACCAGTCCA-3'
P11	TR-f	5'- AA*GCTAGC***ATG**TATATGCGCCCGGCGATTGCAGTTCCACTG-3'

[a]The introduced restriction sites are shown in italics. The start codons are in bold.

Table S2. Plasmid constructs and the resulting protein products.

Plasmid	Vector Source	Genes	Marker	Protein products
pKJ75	pET23a	*nrps325*	*Amp*	C-terminal hexahistidine tagged NRPS325
pKJ113	pET23a	*nrps325-H193A*	*Amp*	C-terminal hexahistidine tagged NRPS325-H193A
pKJ114	pET23a	*nrps325-H194A*	*Amp*	C-terminal hexahistidine tagged NRPS325-H194A
pKJ115	pET23a	*nrps325-ATR*	*Amp*	C-terminal hexahistidine tagged ATR
pKJ116	pET23a	*nrps325-TR*	*Amp*	C-terminal hexahistidine tagged TR
pKJ119	pET23a	*nrps325-G1132A-G1135A*	*Amp*	C-terminal hexahistidine tagged NRPS325-G1132A-G1135A

Table S3. NMR Data for **2a**.

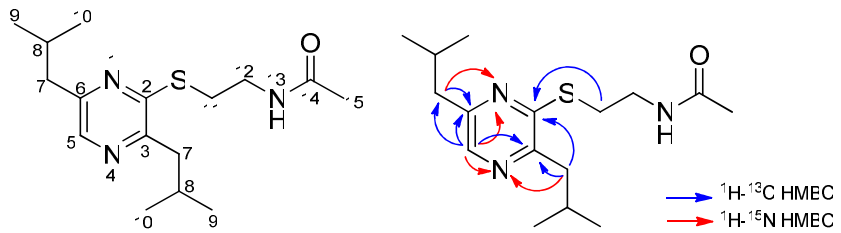

No.	^{13}C δ (ppm)	^{1}H δ (ppm) (m, area, J_{HH} (Hz))	HMBC
1	-	-	-
2	153.9	-	-
3	153.6	-	-
4	-	-	-
5	139.0	8.25 (s, 1H)	C3, C6, C7, N1, N4
6	151.7	-	-
7 7’	44.2 33.1	2.56 (d, 2H, 7.1), 2.57 (d, 2H, 7.1)	C5, C6, C8, C9, C10, N1 C3, C2, C8’, C9’, C10’, N4
8 8’	29.1 27.7	2.09 (m, 1H), 2.19 (m, 1H)	C7, C9, C10 C7’, C9’, C10’
9 10	22.5	0.87 (d, 6H, 6.7)	C7, C8, C9, C10
9’ 10’	22.7	0.89 (d, 6H, 6.6)	C7’, C8’, C9’, C10’
11	29.1	3.29 (t, 2H, 6.7)	C2, C12
12	39.4	3.45 (t, 2H, 6.5)	C11, C14, N13
13	-	7.35 (br, 1H)	-
14	169.69	-	-
15	22.8	1.87 (s, 3H)	C14, N13

Spectra were obtained at 500 MHz for protons and 125 MHz for carbons and were recorded in CD_3COCD_3.

Table S4. Matrices of compounds biosynthesized by NRPS325.

	N-acetylcysteamine $R_2=CH_2NHCOCH_3$	dithiothreitol (DTT) $R_2=CH(OH)CH(OH)CH_2SH$	mercaptoethanol $R_2=CH_2OH$	4-mercapto-1-butanol $R_2=CH_2CH_2CH_2OH$
L-Leu $R_1=CH_2CH(CH_3)_2$	**2a**, 100%[a]	**1a**, 52%	**6a**, 60%	**7a**, 36%
L-Val $R_1=CH(CH_3)_2$	**2b**, 18%	**1b**, 14%	**6b**, 9%	**7b**, 8%
L-Met $R_1=CH_2CH_2SCH_3$	**2c**, 51%	**1c**, 50%	**6c**, 39%	**7c**, 25%
L-Ile $R_1=CH(CH_3)CH_2CH_3$	**2d**, 45%	**1d**, 32%	**6d**, 17%	**7d**, 22%
L-Phe $R_1=CH_2Ph$	**2e**, 71%	**1e**, 29%	**6e**, 29%	**7e**, 19%
L-Tyr $R_1=CH_2PhOH$	**2f**, 59%	**1f**, 31%	**6f**, 20%	**7f**, 16%
Tfl $R_1=CH_2CH(CH_3)CF_3$	**2g**, 19%	**1g**, 23%	**6g**, 29%	**7g**, 30%
Aha $R_1=CH_2CH_2N_3$	**2h**, 25%	**1h**, 36%	**6h**, 17%	**7h**, 26%
L-Trp $R_1=C_9H_8N$[b]	**2i**, 10%	**1i**, 9%	**6i**, 10%	**7i**, 11%

	1-mercapto-2-propanol $R_2=CH(OH)CH_3$	3-mercapto-1-propanol $R_2=CH_2CH_2OH$	methyl 3-mercaptopropionate $R_2=CH_2COOCH_3$
L-Leu $R_1=CH_2CH(CH_3)_2$	**8a**, 43%	**9a**, 50%	**10a**, 11%
L-Val $R_1=CH(CH_3)_2$	**8b**, 20%	**9b**, 9%	**10b**, 4%
L-Met $R_1=CH_2CH_2SCH_3$	**8c**, 36%	**9c**, 41%	**10c**, 15%
L-Ile $R_1=CH(CH_3)CH_2CH_3$	**8d**, 33%	**9d**, 21%	**10d**, 13%
L-Phe $R_1=CH_2Ph$	**8e**, 41%	**9e**, 31%	**10e**, 11%
L-Tyr $R_1=CH_2PhOH$	**8f**, 42%	**9f**, 23%	**10f**, 9%
Tfl $R_1=CH_2CH(CH_3)CF_3$	**8g**, 20%	**9g**, 31%	**10g**, 17%
Aha $R_1=CH_2CH_2N_3$	**8h**, 39%	**9h**, 21%	**10h**, 16%
L-Trp $R_1=C_9H_8N$[b]	**8i**, 12%	**9i**, 13%	**10i**, 6%

[a]: The percentages in parenthesis indicate the relative yields of pyrroles and pyrazines normalized to the yields of **1a** and **2a**, respectively.

[b]: $C_9H_8N=$ 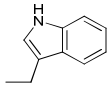

2.2. Supplementary Figures

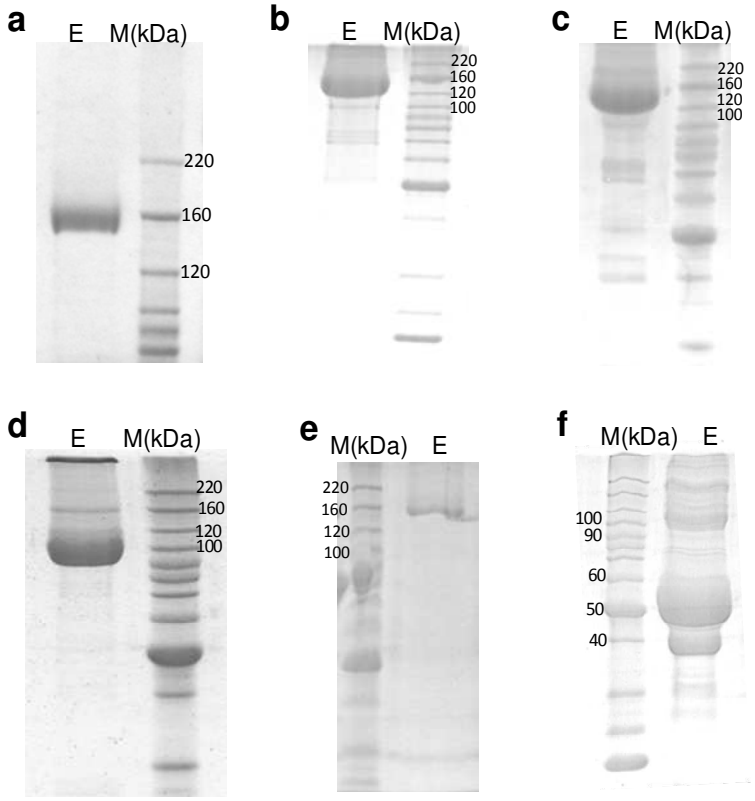

Figure S1. SDS-PAGE gels of proteins purified from *E. coli* BAP1 and BL21(DE3). (a) 6% SDS-PAGE gel of C-terminal hexahistidine tagged NRPS325 (158 kDa) from *E. coli* BAP1 after Ni-NTA chromatography. (b) 12% SDS-PAGE gel of C-terminal hexahistidine tagged NRPS325-H193A (158 kDa) from *E. coli* BAP1 after Ni-NTA chromatography. (c) 12% SDS-PAGE gel of C-terminal hexahistidine tagged NRPS325-H194A (158 kDa) from *E. coli* BAP1 after Ni-NTA chromatography. (d) 12% SDS-PAGE gel of C-terminal hexahistidine tagged ATR (107 kDa) from *E. coli* BAP1 after Ni-NTA chromatography. (e) 12% SDS-PAGE gel of C-terminal hexahistidine tagged NRPS325-G1132A-G1135A (158 kDa) from *E. coli* BAP1 after Ni-NTA chromatography. (f) 12% SDS-PAGE gel of C-terminal hexahistidine tagged TR (51 kDa) from *E. coli* BAP1 after Ni-NTA chromatography (there is a 40 kDa truncated R domain existed). In all the gels, lane M: Invitrogen Benchmark Protein Ladder, Lane E: Final elution of protein after chromatography.

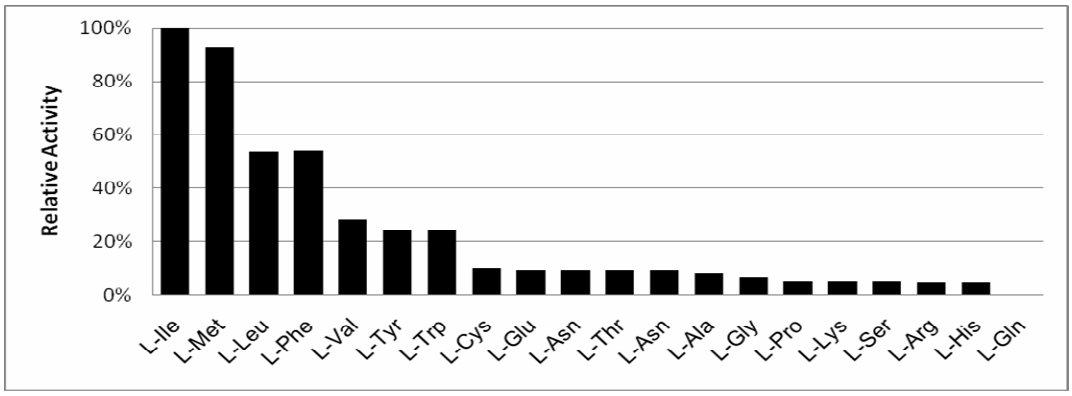

Figure S2. Relative activities of NRPS325 towards different amino acid substrates as determined by the PPi releasing assay. The y axis indicates the relative activity for various amino acids compared to the activity for L-isoleucine (100% activity). The activity of NRPS325 towards different amino acids was determined by the measurement of released PPi in the reaction containing 1 µM NRPS325, 2 mM L-amino acid, 75 mM Tris-HCl (pH 7.5), 10 mM $MgCl_2$, 5 mM ATP and 33µL pyrophosphate reagent from Sigma-Aldrich (See Experimental Methods). PPi levels were measured by monitoring the disappearance of NADH (340 nm). The spectrophotometer recorded data points every 20 s. The reaction initial velocities were calculated by using a minimum of 20 co-linear data points and an extinction coefficient of 6400 $M^{-1}cm^{-1}$ for NADH.

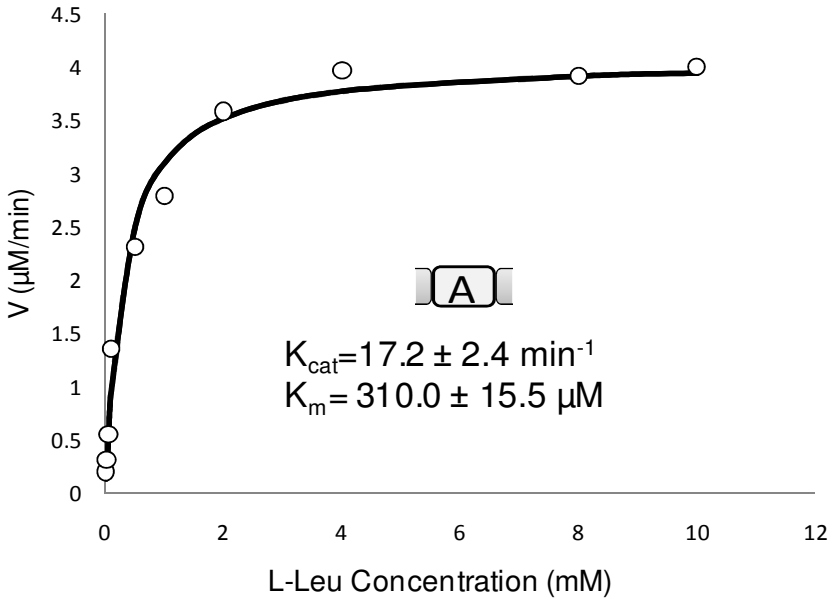

Figure S3. Kinetic analysis of NRPS325 catalyzed formation of L-leucyl-AMP. Reaction (100 μL) contains 75 mM Tris-HCl (pH=7.5), 10 mM $MgCl_2$, 5 mM ATP and was incubated with 500 nM NRPS325 in the presence of various concentrations (from 20 μM to 10 mM) of L-leucine at 25 °C. The released PPi levels were measured by monitoring the disappearance of NADH (at 340 nm) in the continuous spectrophotometric assay with 33 μL Pyrophosphate Reagent (Sigma-Aldrich). The spectrophotometer recorded data points every 20 s. The reaction initial velocities were calculated by using a minimum of 20 co-linear data points and an extinction coefficient of 6400 $M^{-1}cm^{-1}$ for NADH.

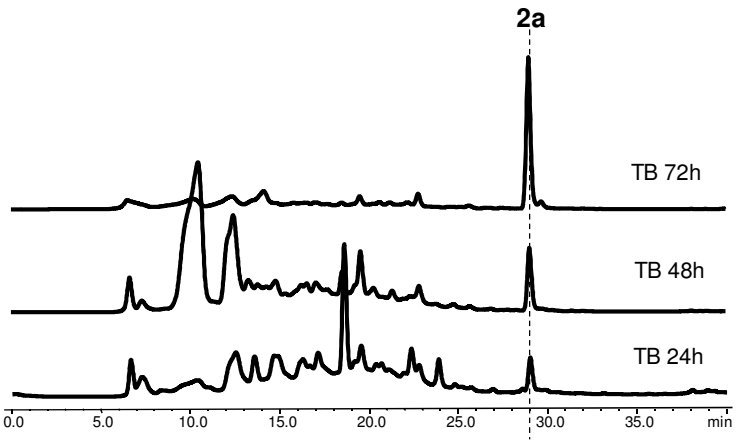

Figure S4. LC-MS traces for the in vivo production of **2a** with *E. coli* BAP1/pKJ75 in Terrific Broth media. Feeding *E. coli* BAP1 containing NRPS325 expression plasmid with the free thiol molecule NAC lead to the production of compound **2a**. The maximum yield of compound **2a** (30 mg/L) was reached when implemented 5 mM NAC into TB media after 72 h's growth.

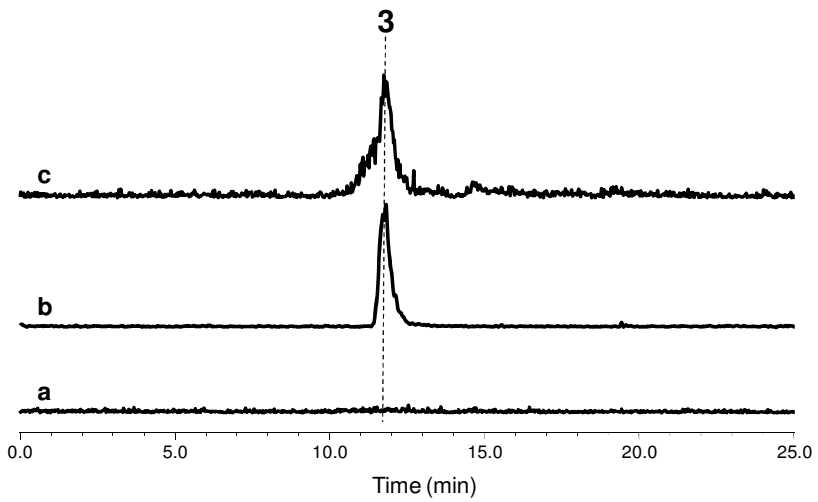

Figure S5. LC-MS traces for the appearance of leucyl-*S*-NAC **3** when NRPS325 is incubated with L-leucine in the presence of ATP and NADPH. (a) Mass filter of *m/z* $[M+H]^+$ 233 in the assay without NRPS325. (b) Mass filter of m/z $[M+H]^+$ 233 of standard **3**. (c) Mass filter of m/z $[M+H]^+$ 233 in the NRPS325 assay. Authentic standard of leucyl-*S*-NAC **3** was synthesized according to the standard procedure.[2] Reactions (100 µL) were incubated at 25 °C for 12 h with 10 mM L-Leucine, 10 mM ATP and 2 mM NADPH in the presence or absence of 10 µM NRPS325. The reaction mixtures were quenched and extracted in pure EA and analyzed by LC-MS.

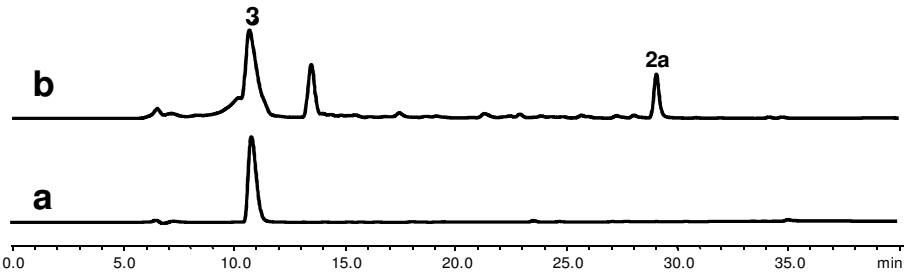

Figure S6. LC-MS traces for the turnover of leucyl-*S*-NAC **3** by NRPS325. (a) Compound **2a** was not produced in the control assay without NRPS325. (b) Production of compound **2a** in the assay containing NRPS325 and NADPH. Reactions (100 μL) were carried out at 25 °C with 10 mM leucyl-*S*-NAC **3**, 2 mM NADPH in the presence or absence of 10 μM NRPS325. The reactions were incubated for 12 h and extracted with pure EA and analyzed by LC-MS.

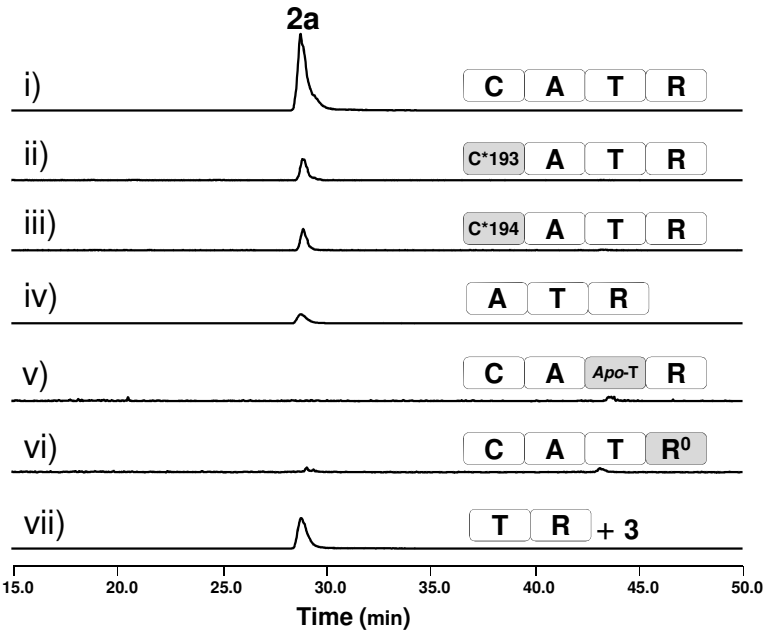

Figure S7. Synthesis of **2a** by intact NRPS325 or dissociated NRPS domains. Traces shown are the selected ion monitoring of desired ion (m/z = 310) in the positive ionization mode. Intensity of the peaks in *vii* was amplified on purpose by 100-fold for clear presentation. Products recovered from in vitro assay with i) NRPS325, ii) NRPS mutant 193, iii) NRPS325 mutant 194, iv) NRPS325-G1132A-G1135A, v) *apo*-NRPS325 in the presence of L-Leu, NAC, ATP and NADPH. The final concentrations of the different components, when added, were: 10 μM enzyme; NAC: 5 mM; L-Leu: 10 mM; NADPH: 2 mM; and ATP: 20 mM. All reactions were performed at room temperature for 12 hr in phosphate buffer (pH=7.4).

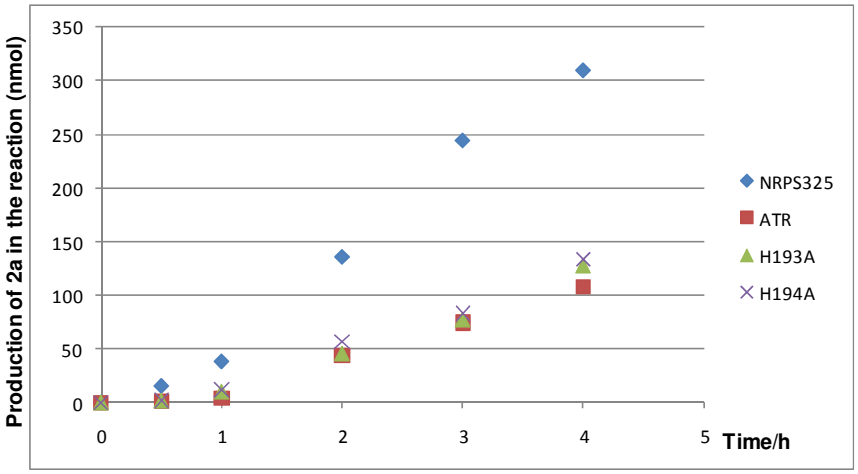

enzyme	Observed Rate (mM/h)
NRPS325	0.616
NRPS325-H193A	0.066
NRPS325-H194A	0.071
325ATR	0.054

Figure S8. Rate of **2a** formation by NRPS325 and variants. The observed rate of **2a** formation was measured using 100 µL reaction mixtures containing 10 µM of enzyme, 5 mM NAC, 10 mM L-Leucine, 10 mM $MgCl_2$, 20 mM ATP and 2 mM NADPH in phosphate buffer. Reactions were initiated by adding enzyme and incubated at room temperature 25°C. The reactions were quenched at 30 min, 1 hour, 2 hour, 3 hour and 4 hour respectively and analyzed by HPLC. The Table below lists the calculated observed formation rate of **2a** at time point 1 h.

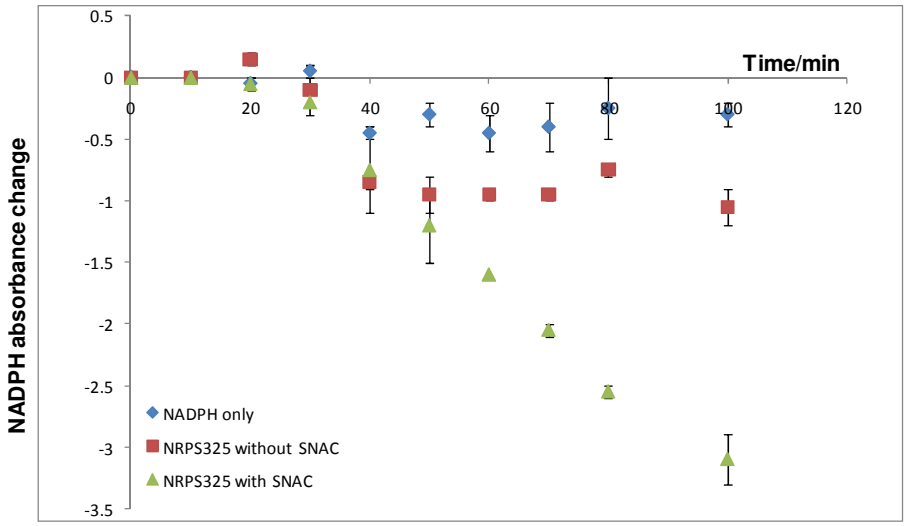

Figure S9. NADPH detection assays**.** 10 μM of NRPS325 was incubated with 10 mM L-Leucine, 10 mM $MgCl_2$, 20 mM ATP and 2 mM NADPH in the presence (green) and absence (red) of 5 mM NAC in phosphate buffer. 2 mM NADPH in phosphate buffer was also monitored and served as a control (blue). Reactions initiated with addition of enzyme and record every 10 min.

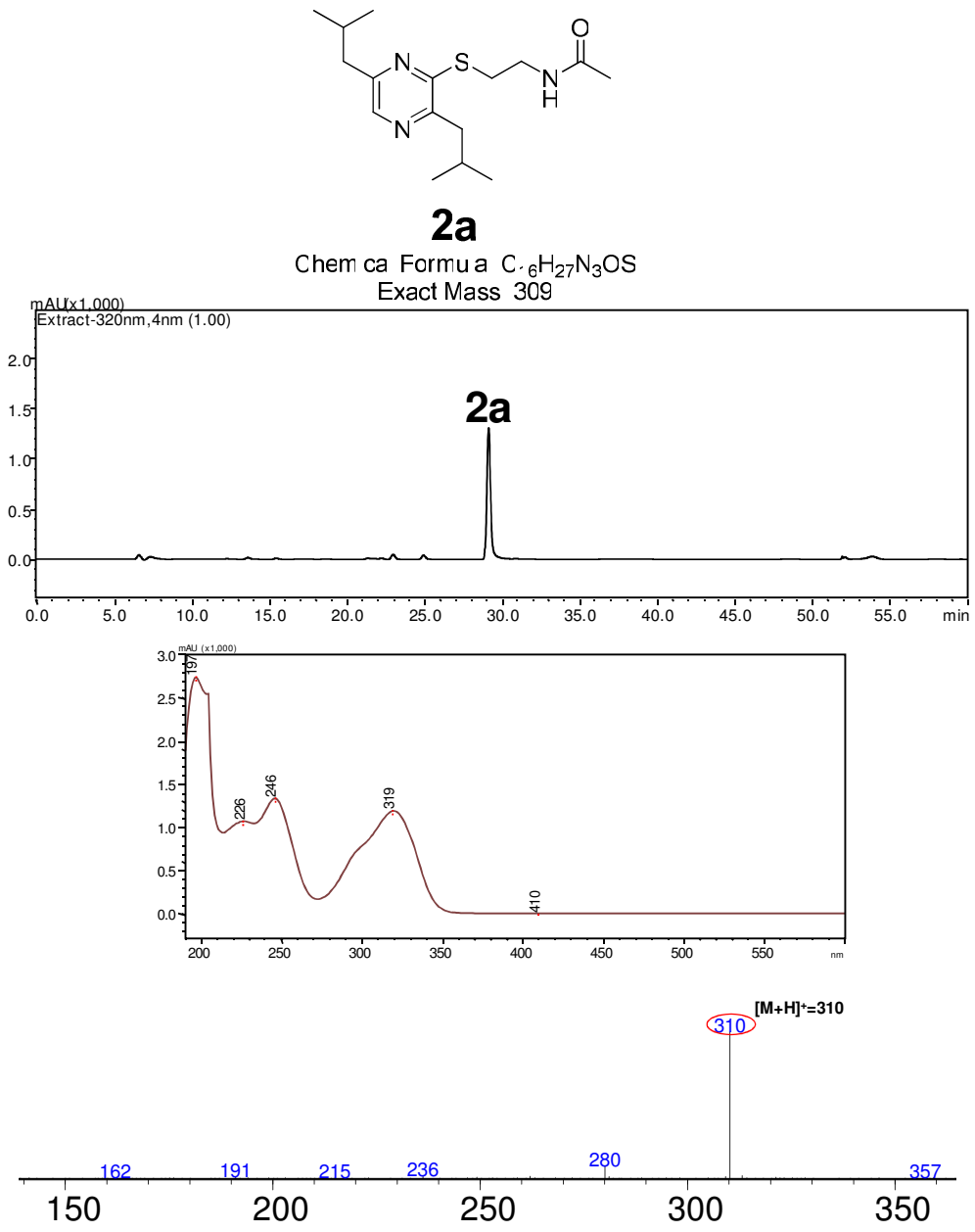

Figure S10. LC-MS and UV data for biosynthesized **2a**. **2a** is synthesized by NRPS325 with L-leucine in the presence of ATP, NAC and NADPH. From top to bottom: LC chromatogram (320nm) showing **2a** as the major compound, the UV absorption of **2a**, positive ($[M+H]^+$) in the ESI-MS spectrum.[3-4]

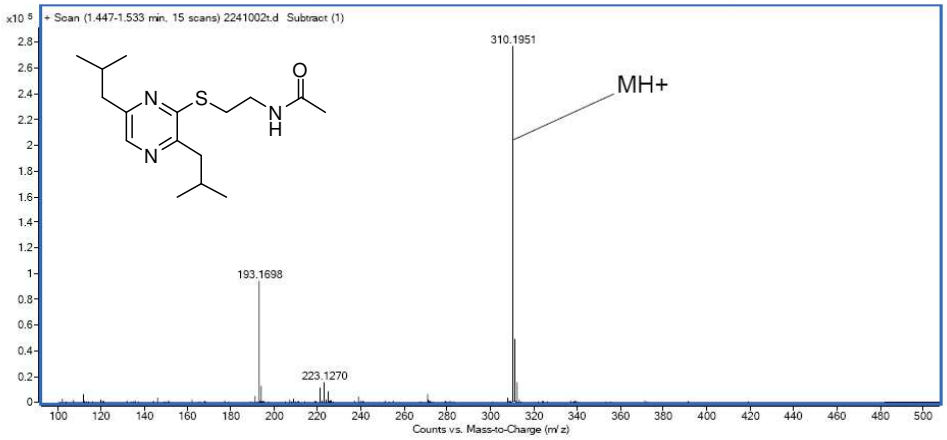

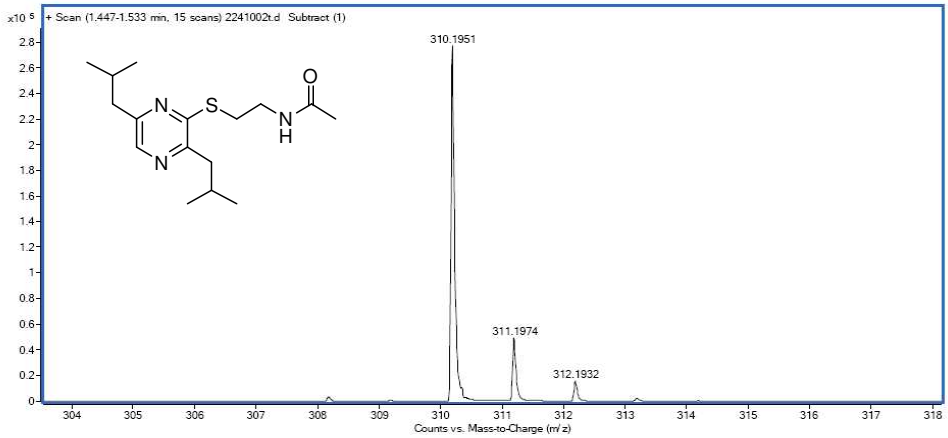

Measured Mass	310.1951	
Element	Low Limit	High Limit
C	11	21
H	15	35
N	0	5
O	0	5
S	0	2

Formula	Calculated Mass	mDaError	ppmError	RDB
C16 H28 N3 O S	310.1948	0.3	1.1	4.5
C18 H30 O2 S	310.1961	-1.0	-3.2	4
C21 H26 O2	310.1927	2.4	7.6	9
C13 H30 N2 O4 S	310.1921	3.0	9.7	0
C13 H32 N3 O S2	310.1981	-3.0	-9.8	-0.5

Figure S11. High-resolution mass spectra (HRMS) for compound **2a** were obtained at the UC Riverside Analytical Chemistry Instrumentation Facility on a VG ZAB2SE FAB spectrometer (Opus V3.1, DEC 3000 Alpha Station). Calculated elemental formula of **2a** was provided based on accurate mass measurement.[3-4]

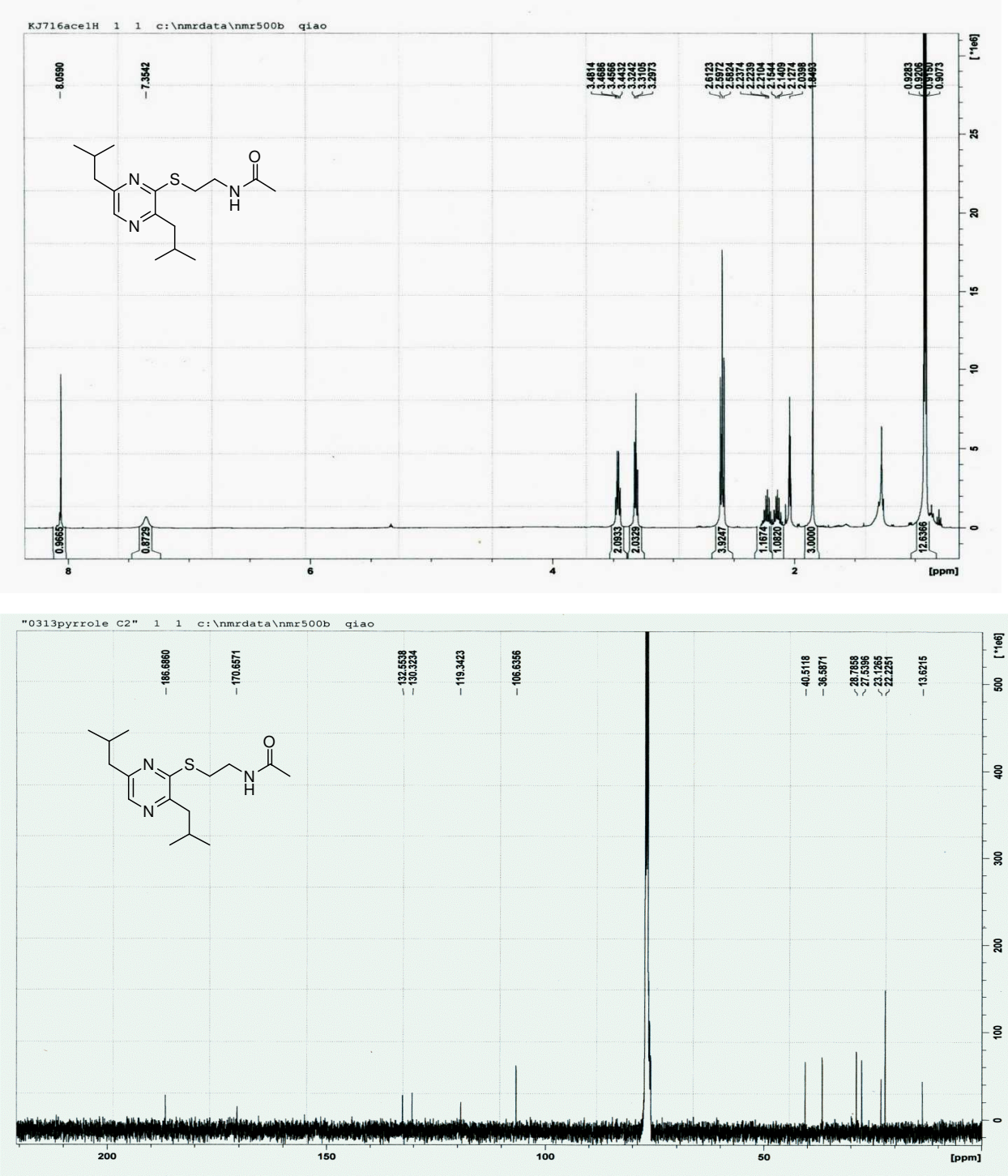

Figure S12. Proton (500 MHz) and carbon (125 MHz) NMR spectra for **2a**. The chemical shift assignments are listed in Table S3.

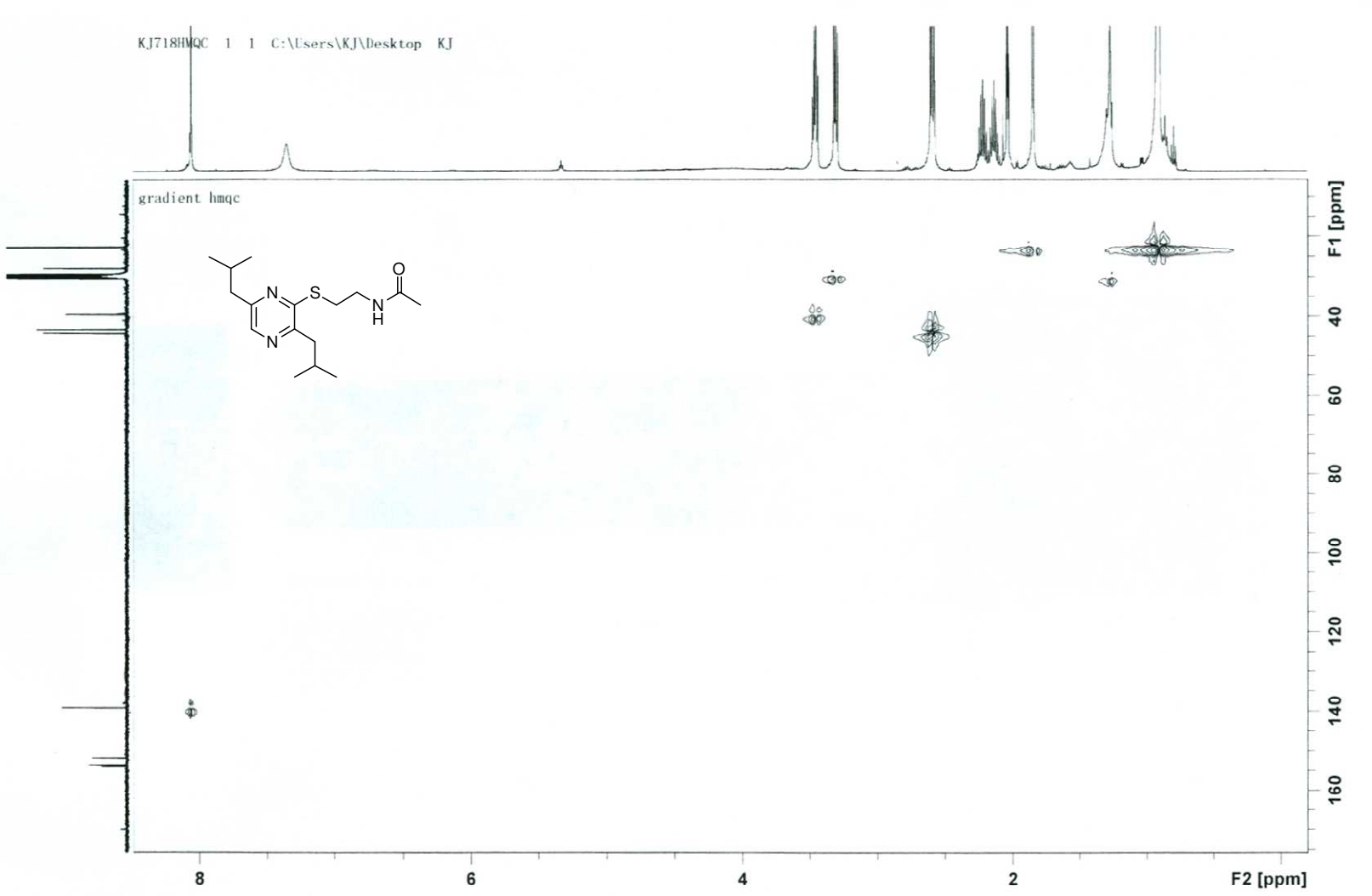

Figure S13. ^{1}H-^{13}C HMQC NMR spectrum for **2a**. The chemical shift assignments are listed in Table S3.

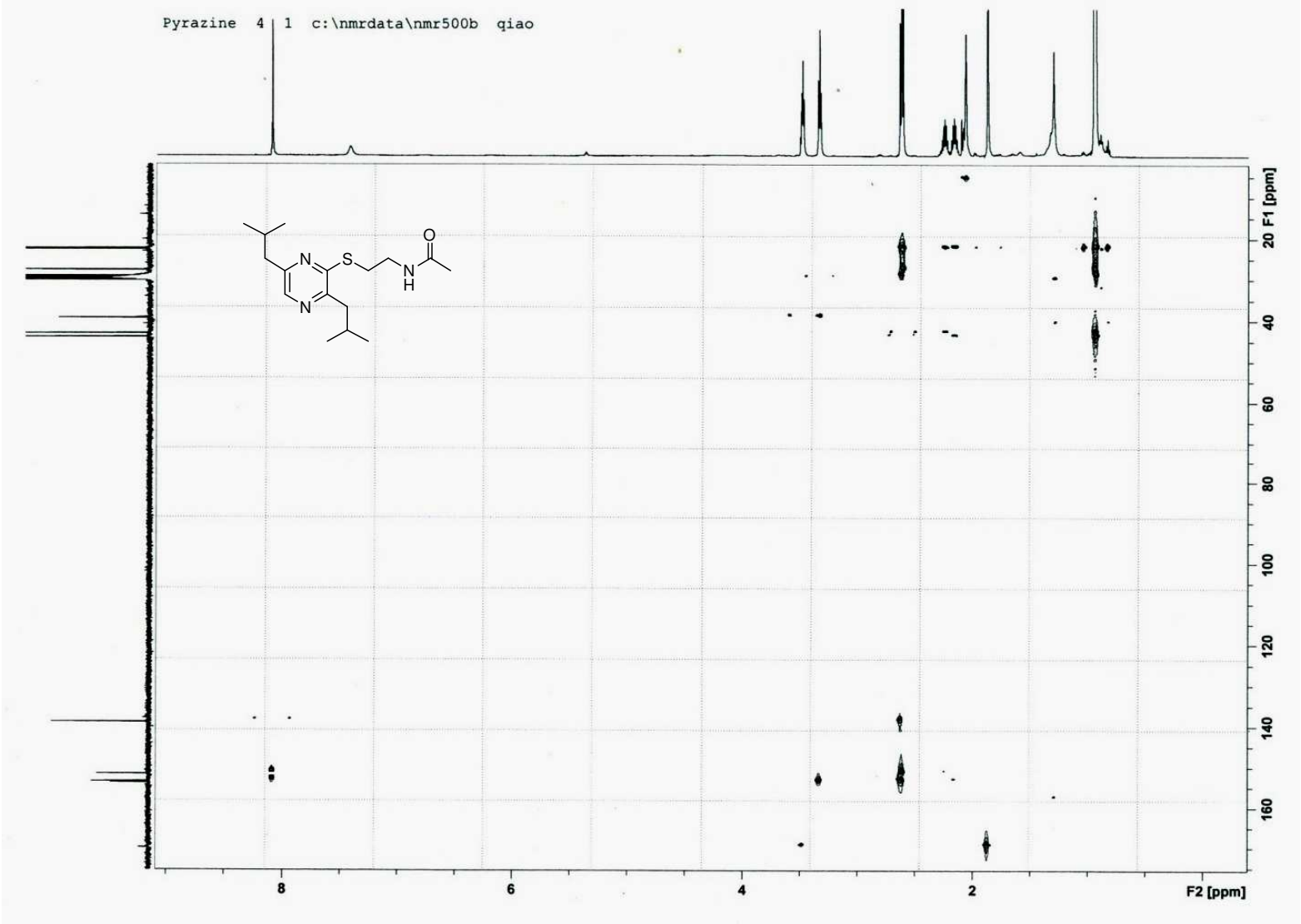

Figure S14. ^{1}H-^{13}C HMBC NMR spectrum for **2a**. The chemical shift assignments are listed in Table S3.

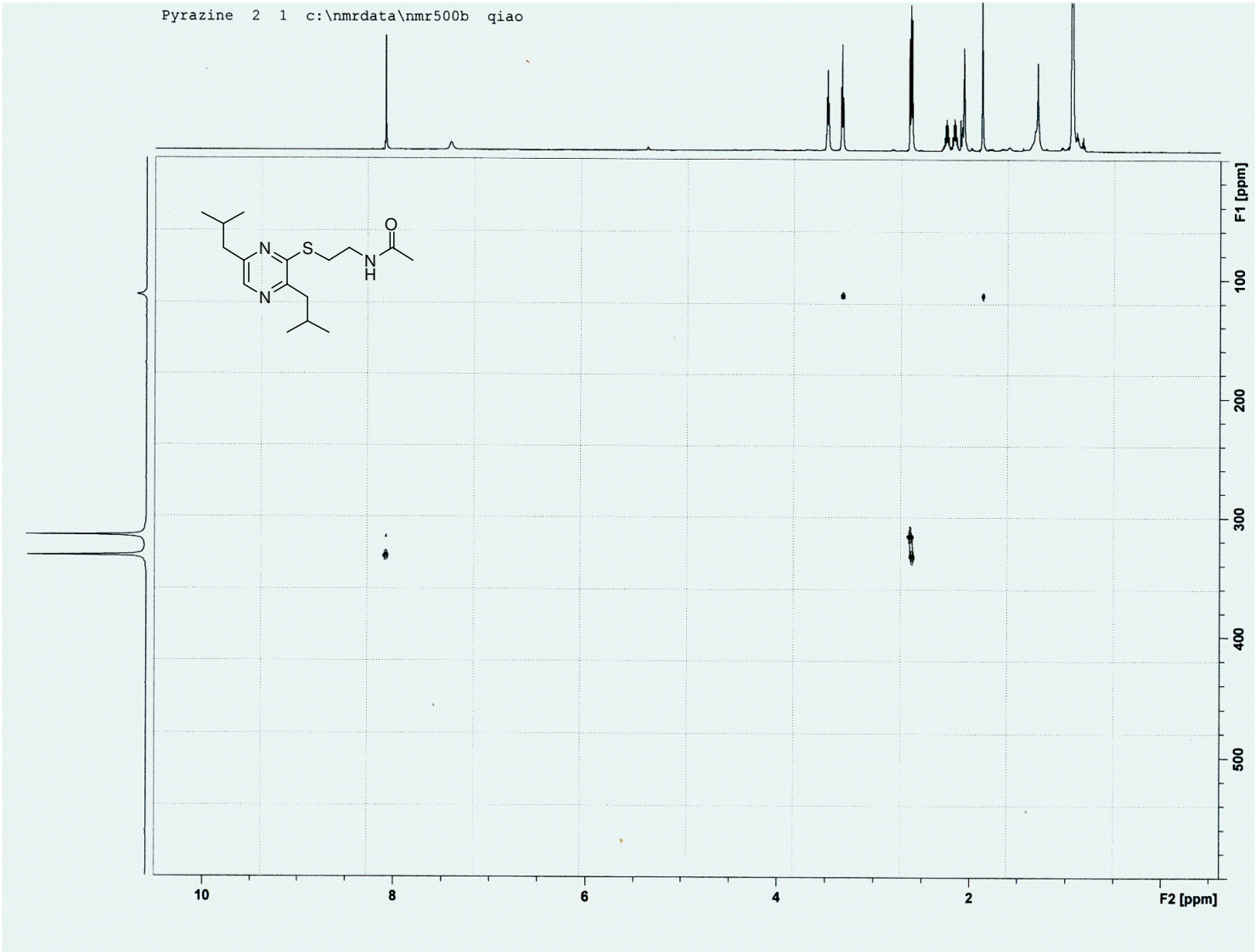

Figure S15. ^{1}H-^{15}N HMBC NMR spectrum for **2a**. The chemical shift assignments are listed in Table S3.

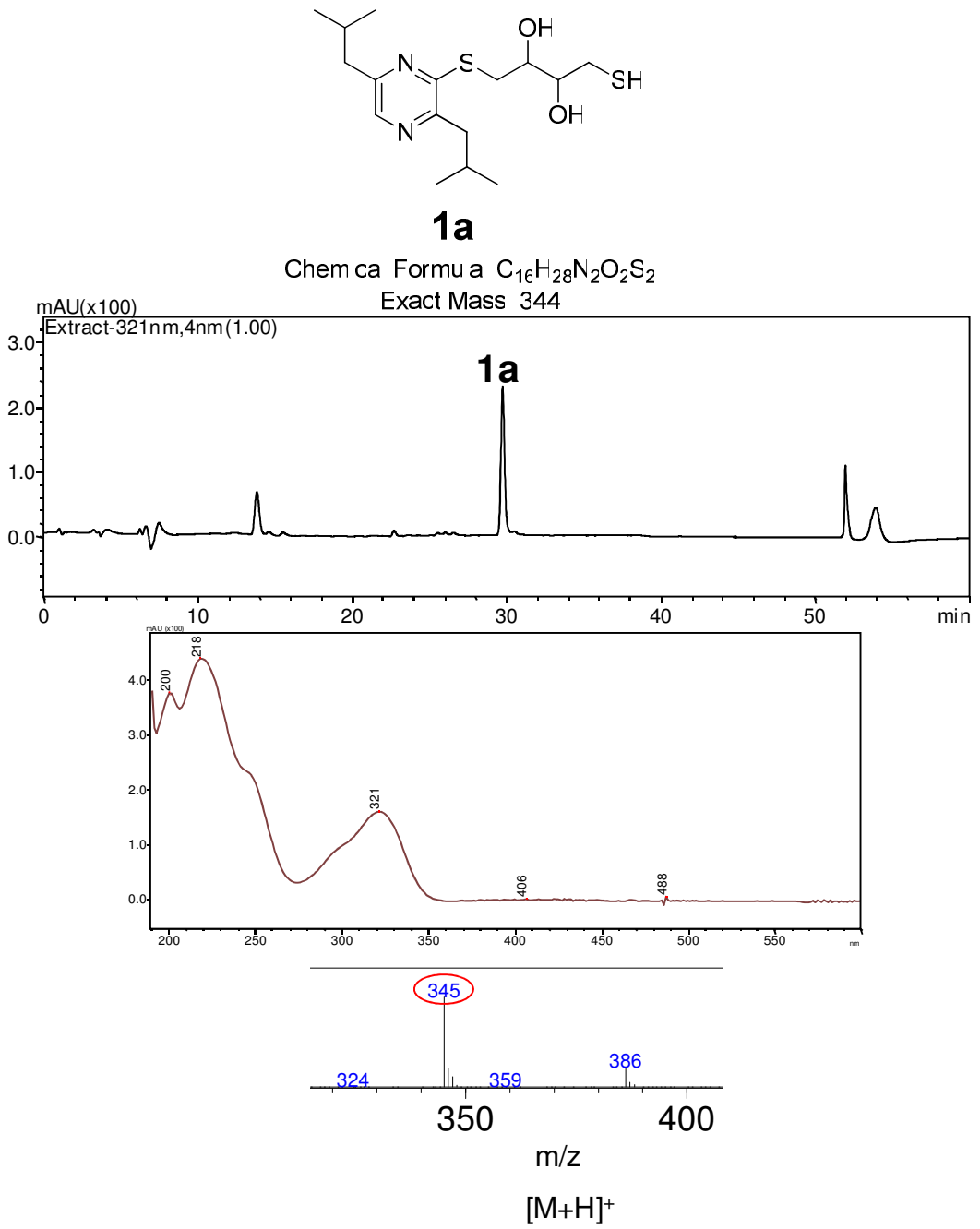

Figure S16. LC-MS and UV data for biosynthesized **1a**. **1a** is synthesized by NRPS325 with L-leucine in the presence of ATP, DTT and NADPH. From top to bottom: LC chromatogram (321nm), the UV absorption of **1a**, positive ($[M+H]^+$) mass ionization in the ESI-MS spectrum.

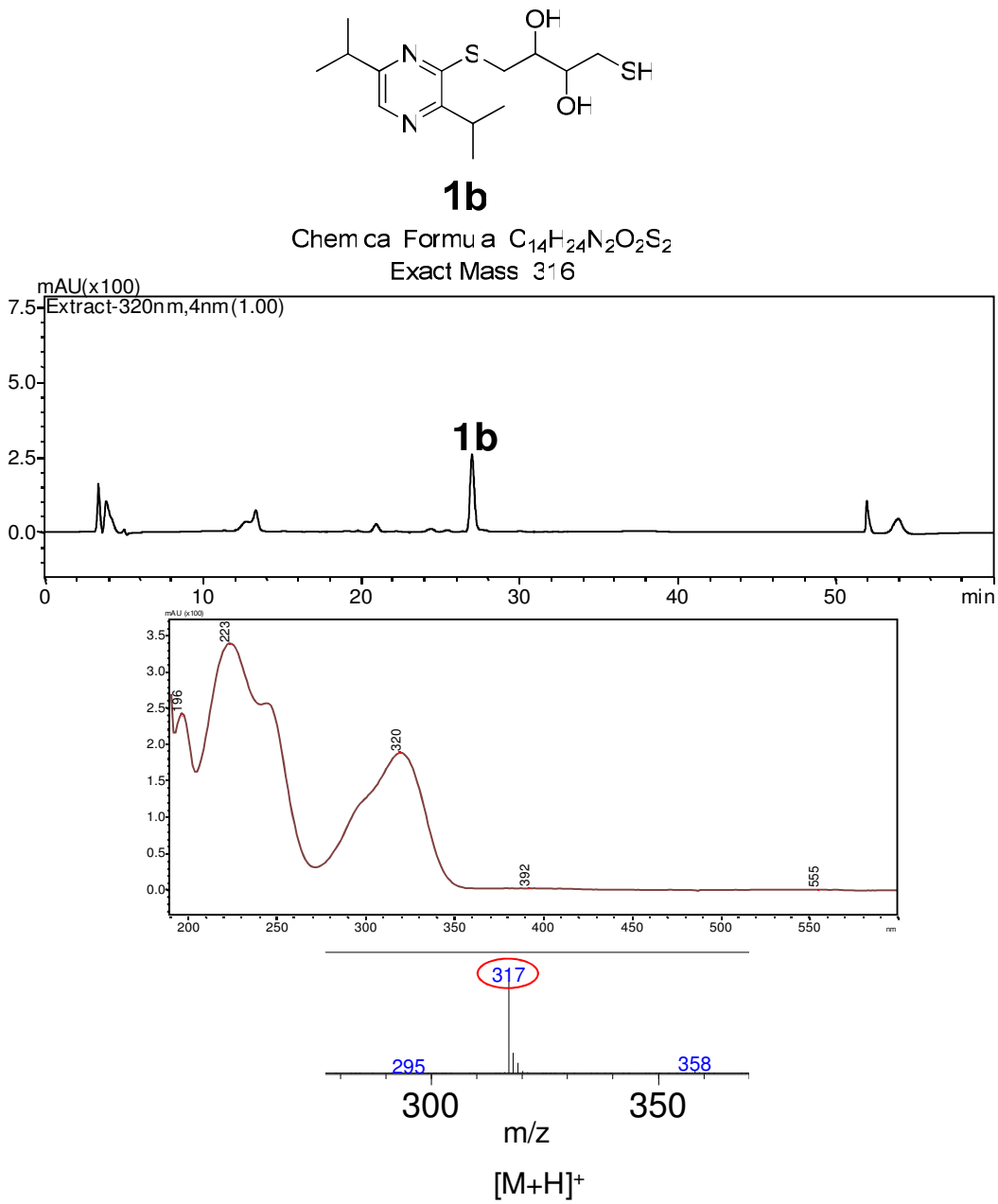

Figure S17. LC-MS and UV data for biosynthesized **1b**. **1b** is synthesized by NRPS325 with L-isoleucine in the presence of ATP, DTT and NADPH. From top to bottom: LC chromatogram (320nm), the UV absorption of **1b**, positive ($[M+H]^+$) mass ionization in the ESI-MS spectrum.

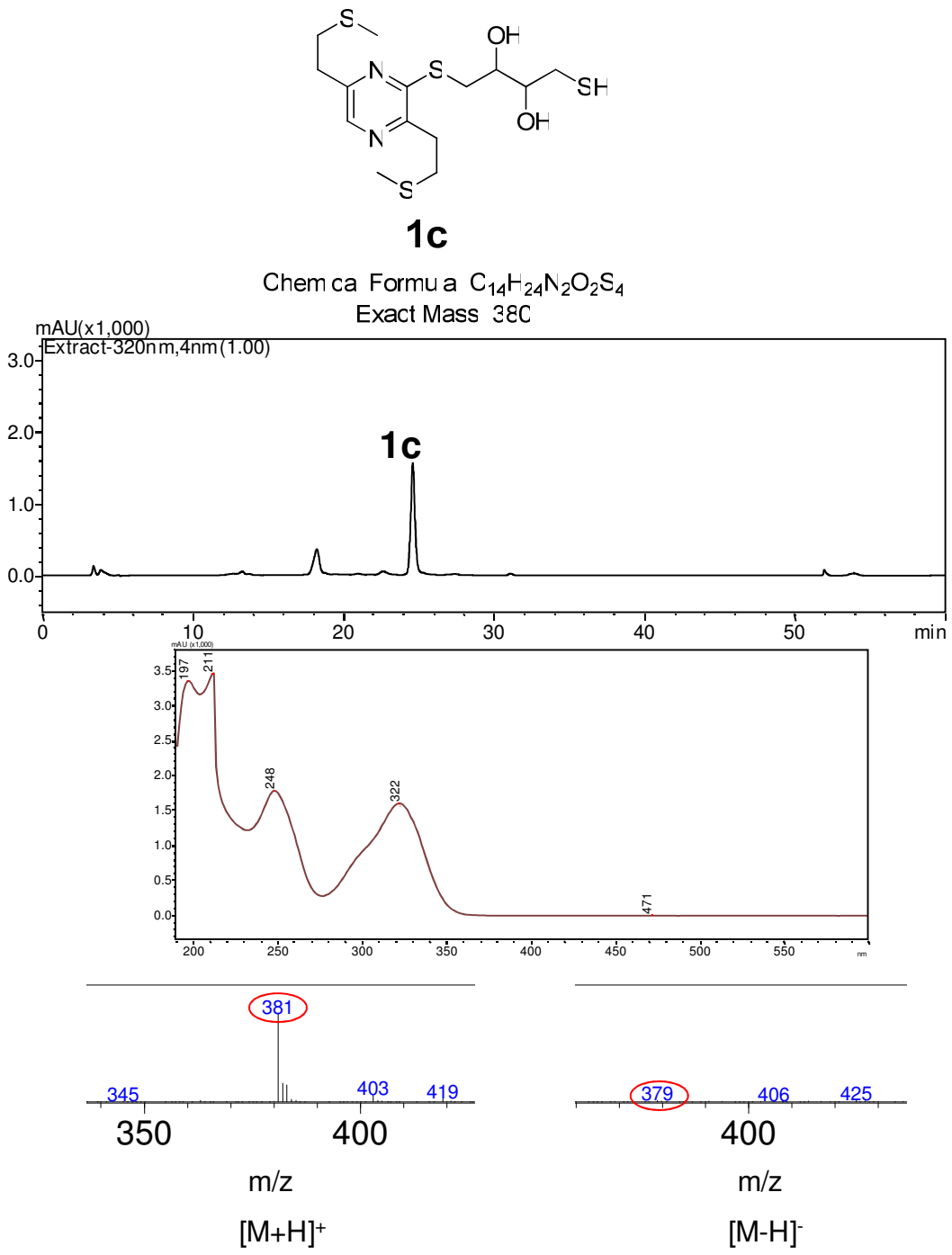

Figure S18. LC-MS and UV data for biosynthesized **1c**. **1c** is synthesized by NRPS325 with L-methionine in the presence of ATP, DTT and NADPH. From top to bottom: LC chromatogram (320nm), the UV absorption of **1c**, positive ($[M+H]^+$ and $[M+Na]^+$) mass ionizations in the ESI-MS spectrum.

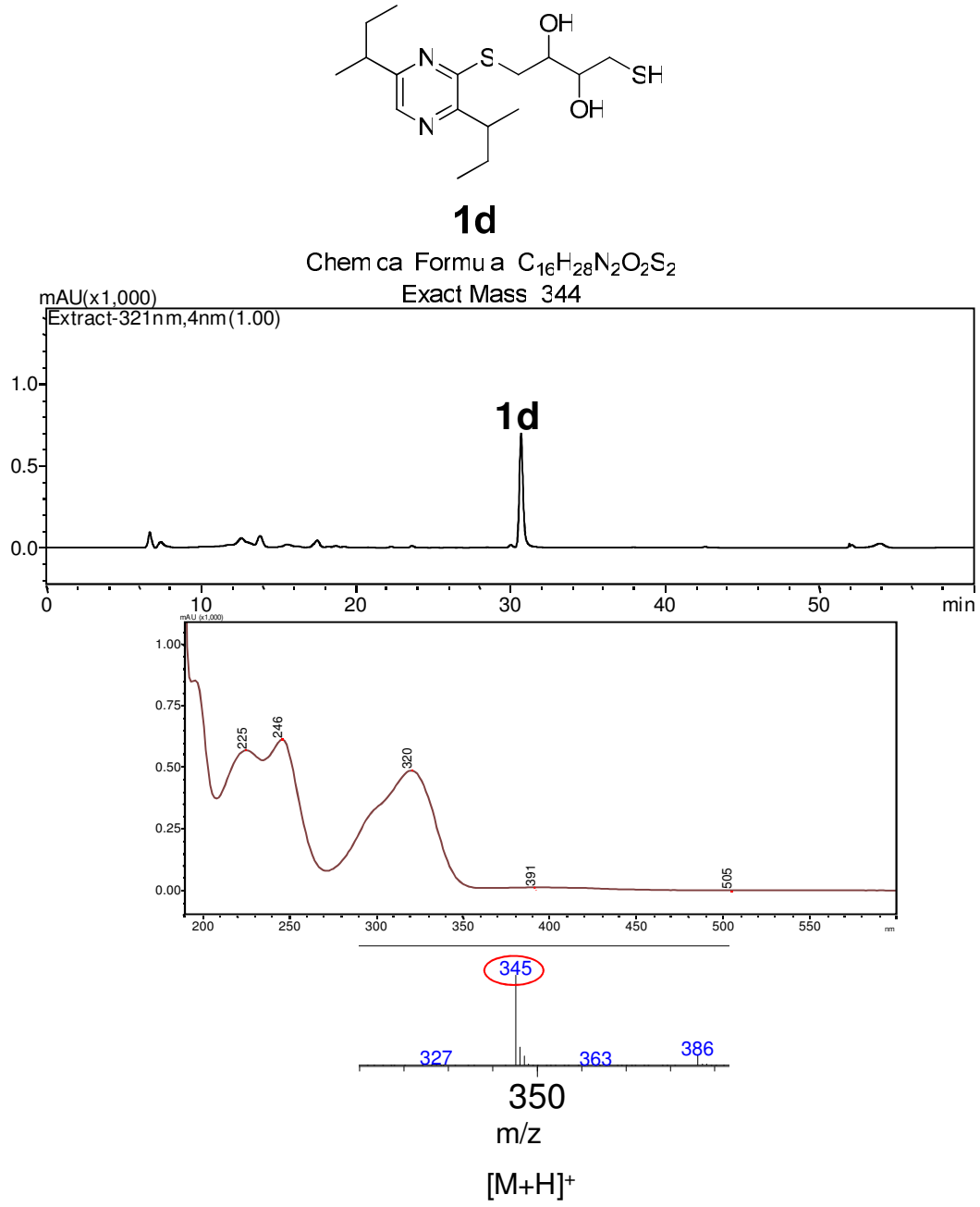

Figure S19. LC-MS and UV data for biosynthesized **1d**. **1d** is synthesized by NRPS325 with L-methionine in the presence of ATP, DTT and NADPH. From top to bottom: LC chromatogram (321nm), the UV absorption of **1d**, positive ($[M+H]^+$) mass ionization in the ESI-MS spectrum.

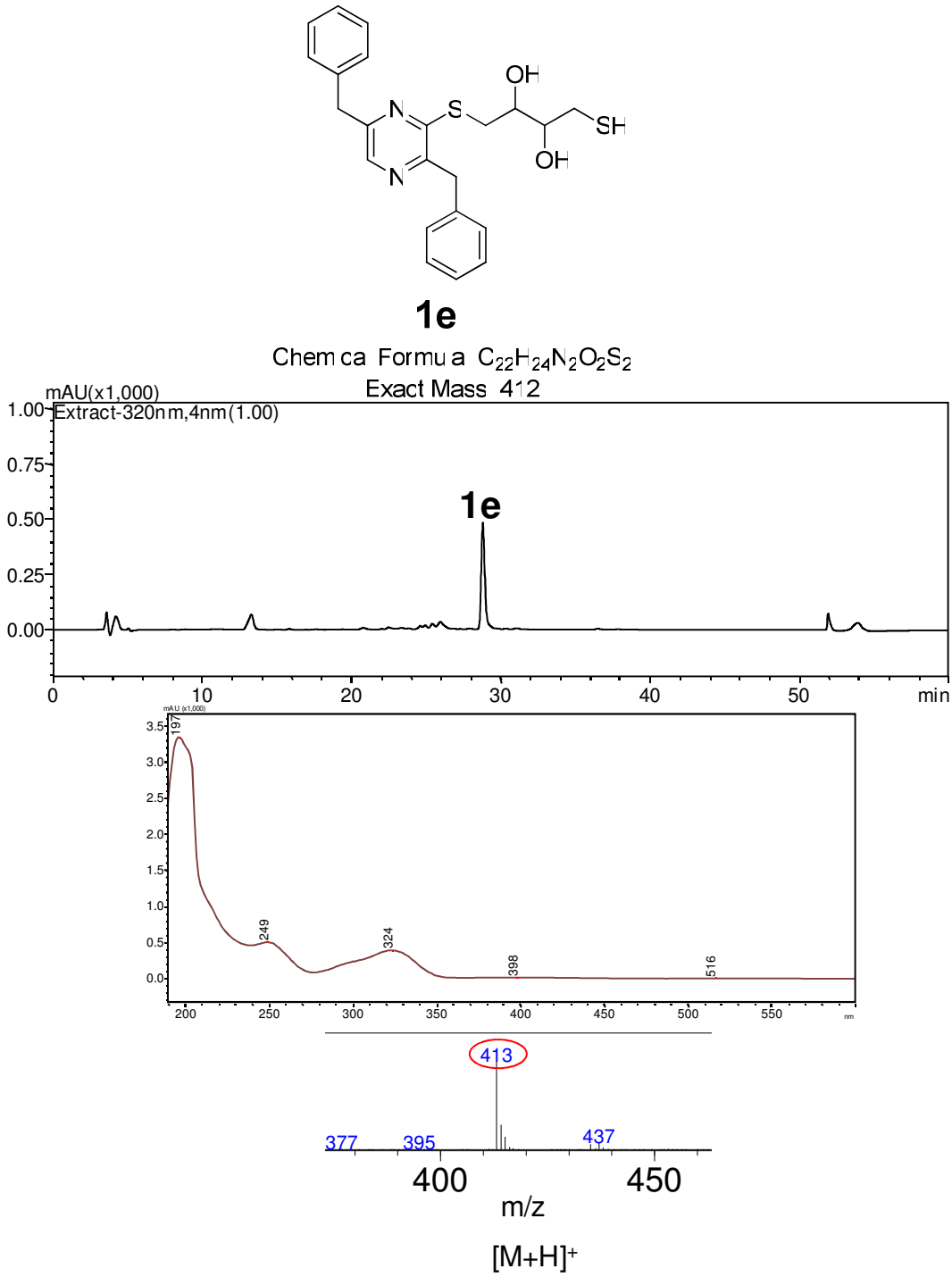

Figure S20. LC-MS and UV data for biosynthesized **1e**. **1e** is synthesized by NRPS325 with L-phenylalanine in the presence of ATP, DTT and NADPH. From top to bottom: LC chromatogram (320nm), the UV absorption of **1e**, positive ($[M+H]^+$) mass ionization in the ESI-MS spectrum.

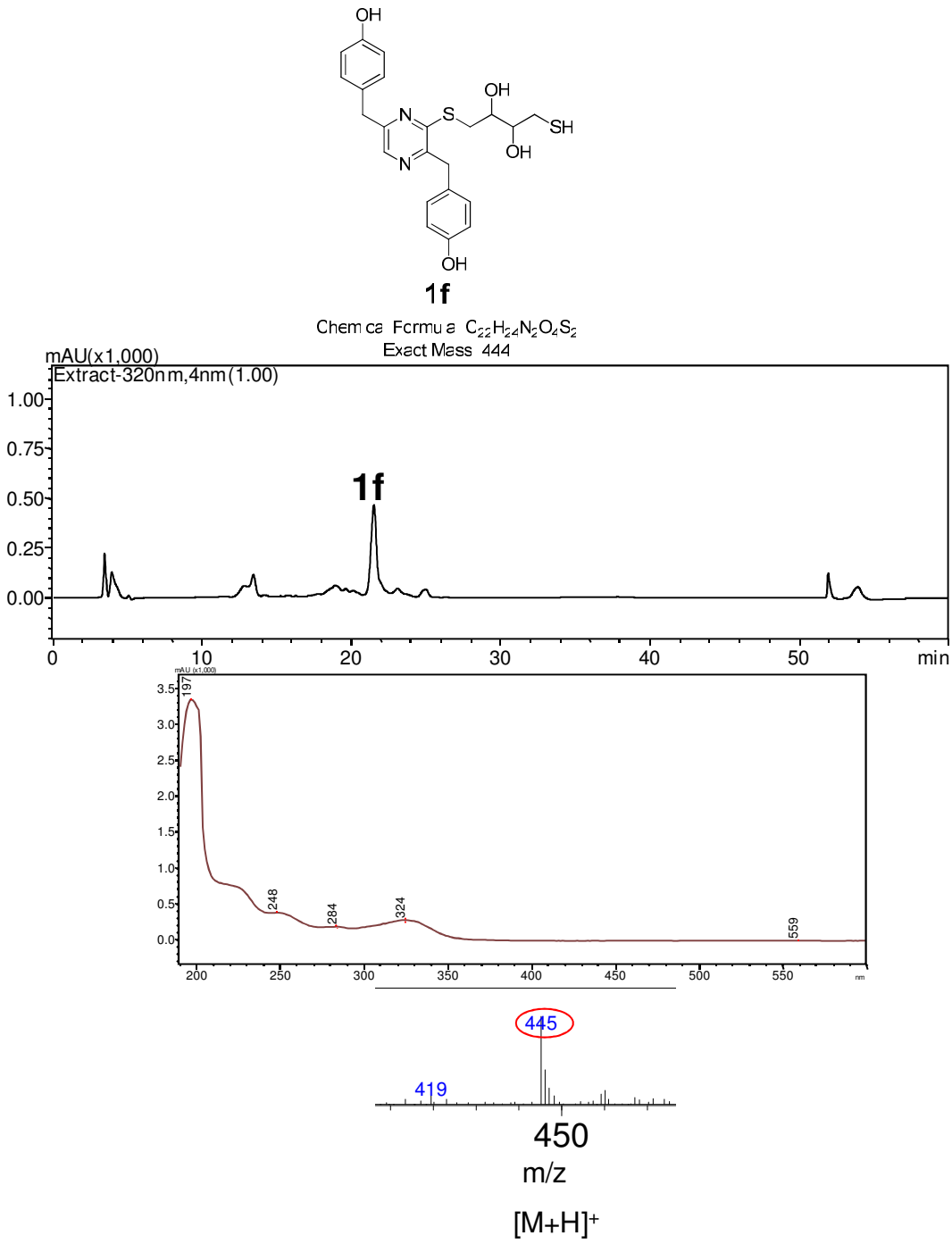

Figure S21. LC-MS and UV data for biosynthesized **1f**. **1f** is synthesized by NRPS325 with L-tyrosine in the presence of ATP, DTT and NADPH. From top to bottom: LC chromatogram (320nm), the UV absorption of **1f**, positive ($[M+H]^+$ and $[M+Na]^+$) mass ionizations in the ESI-MS spectrum.

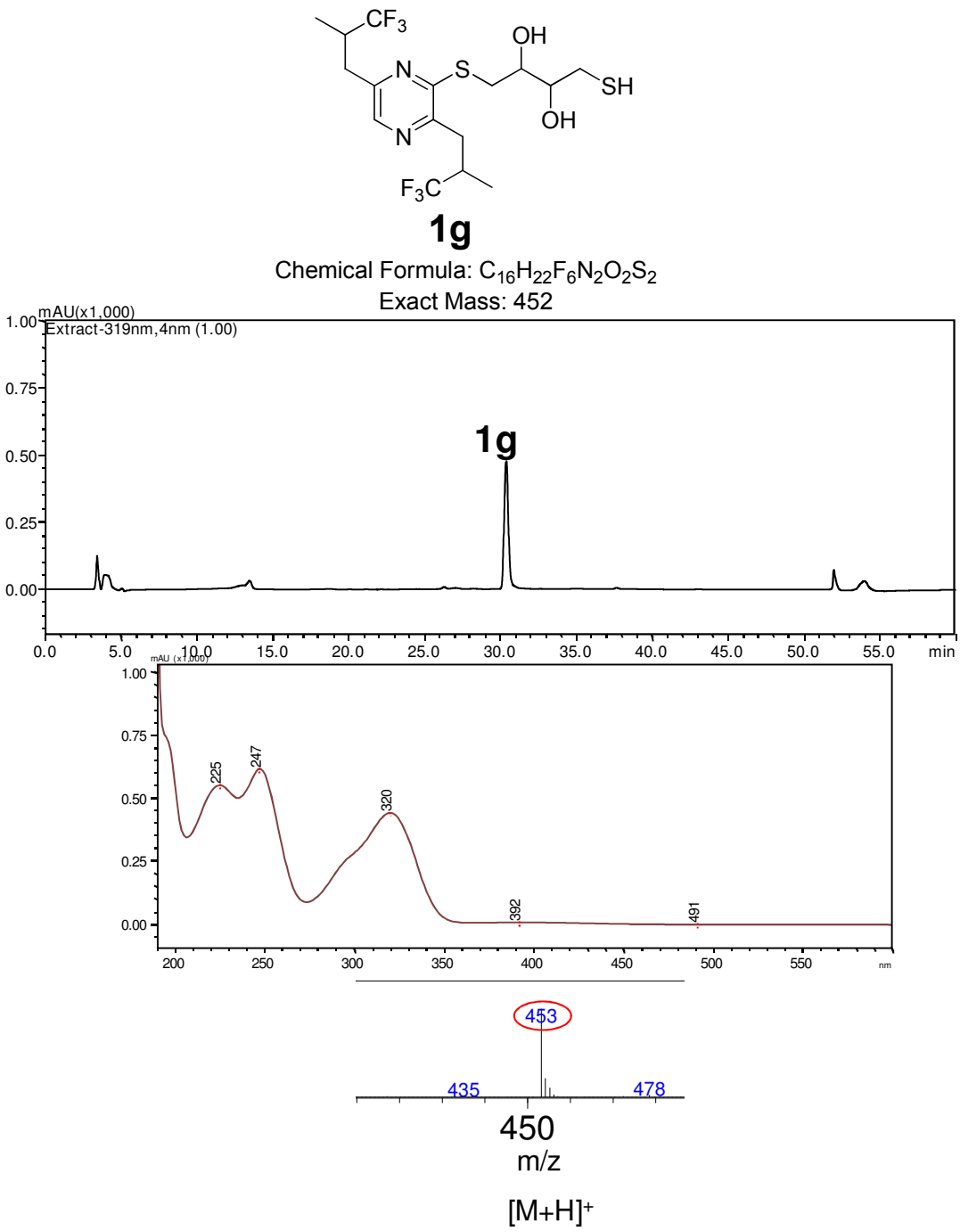

Figure S22. LC-MS and UV data for biosynthesized **1g**. **1g** is synthesized by NRPS325 with trifluoroleucine in the presence of ATP, DTT and NADPH. From top to bottom: LC chromatogram (319nm), the UV absorption of **1g**, positive ($[M+H]^+$) mass ionization in the ESI-MS spectrum.

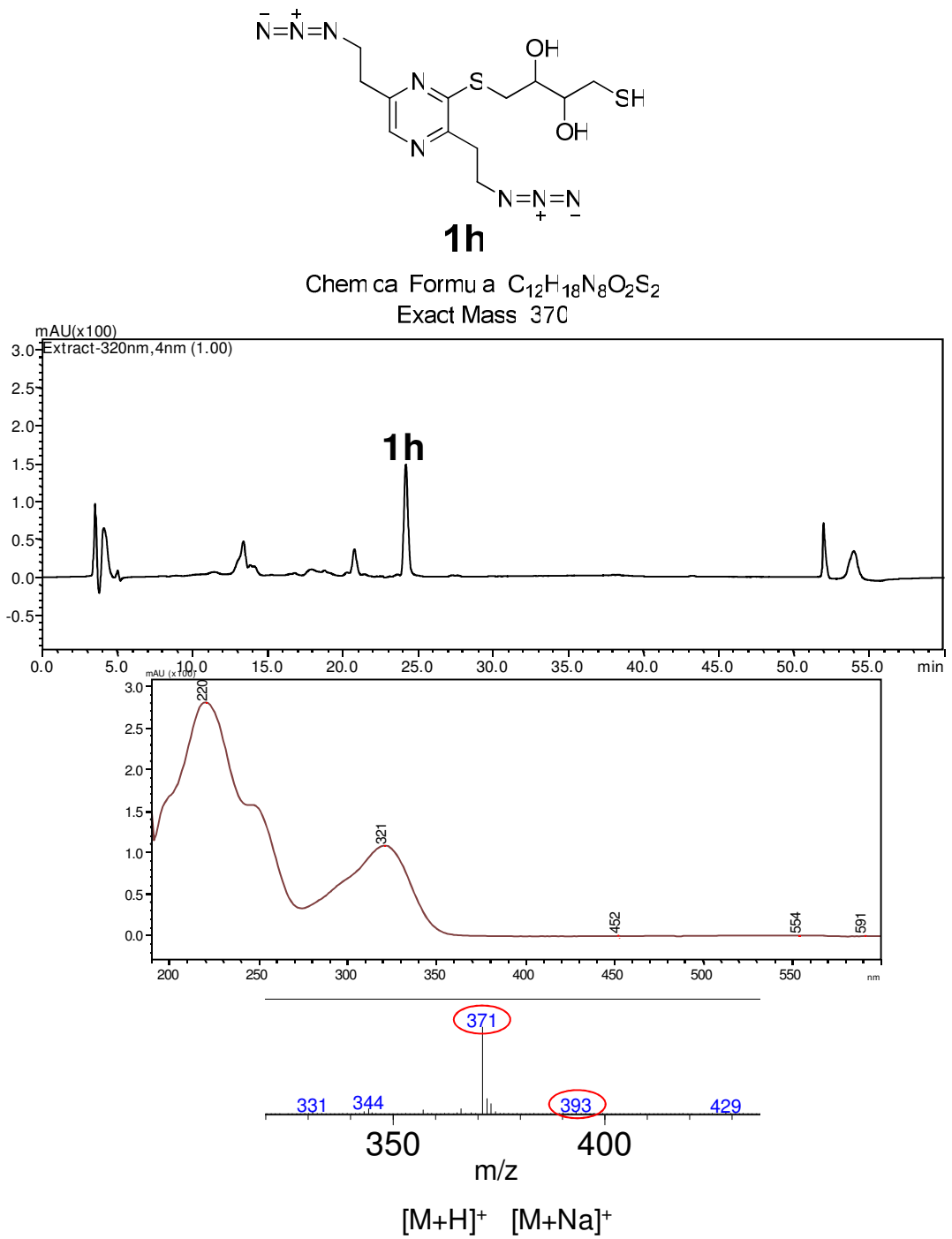

Figure S23. LC-MS and UV data for biosynthesized **1h**. **1h** is synthesized by NRPS325 with azidohomoalanine in the presence of ATP, DTT and NADPH. From top to bottom: LC chromatogram (320nm), the UV absorption of **1h**, positive ($[M+H]^+$ and $[M+Na]^+$) mass ionization in the ESI-MS spectrum.

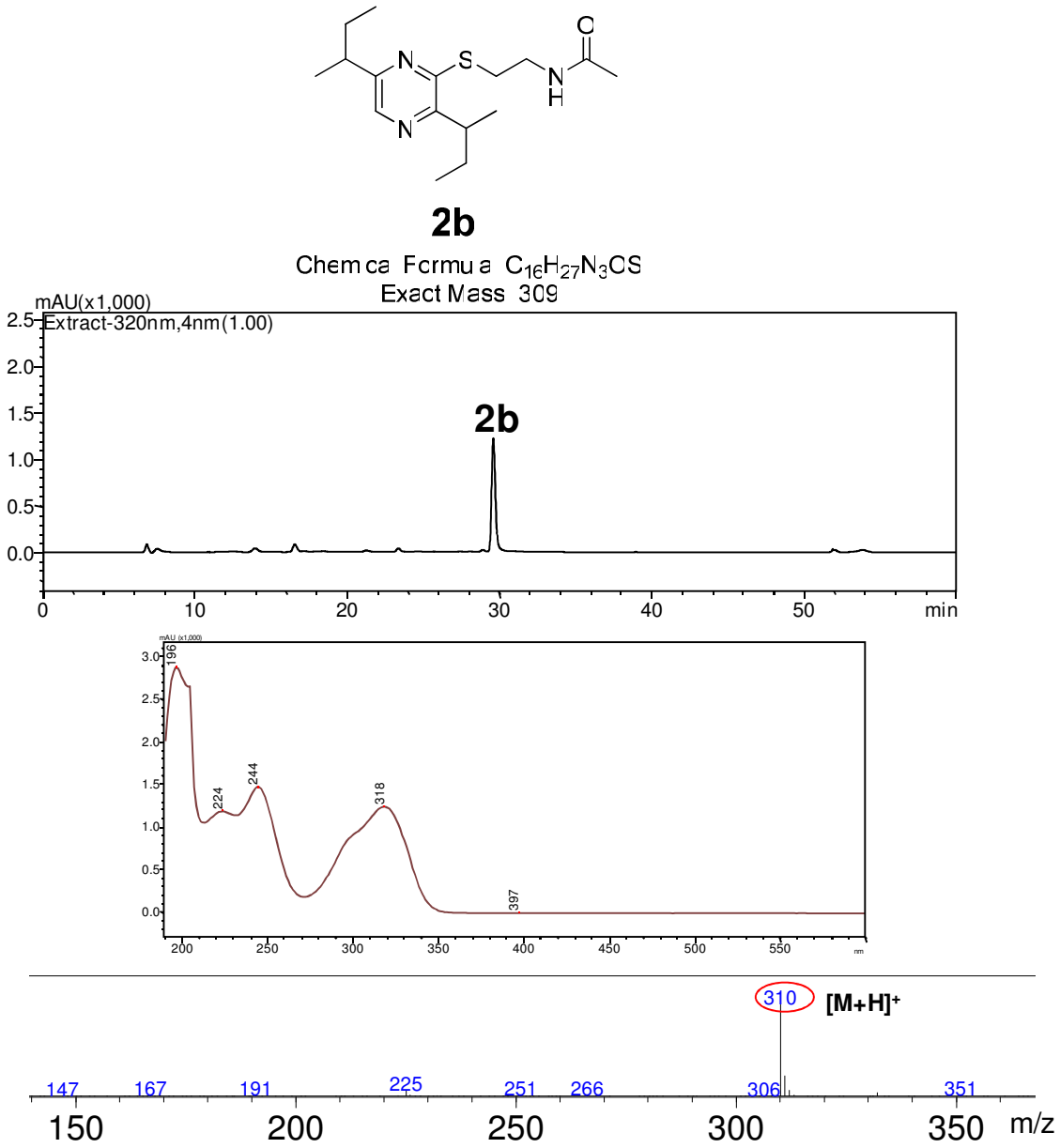

Figure S24. LC-MS and UV data for biosynthesized **2b**. **2b** is synthesized by NRPS325 with L-isoleucine in the presence of ATP, NAC and NADPH. From top to bottom: LC chromatogram (320nm), the UV absorption of **2b**, positive ($[M+H]^+$) mass ionization in the ESI-MS spectrum.

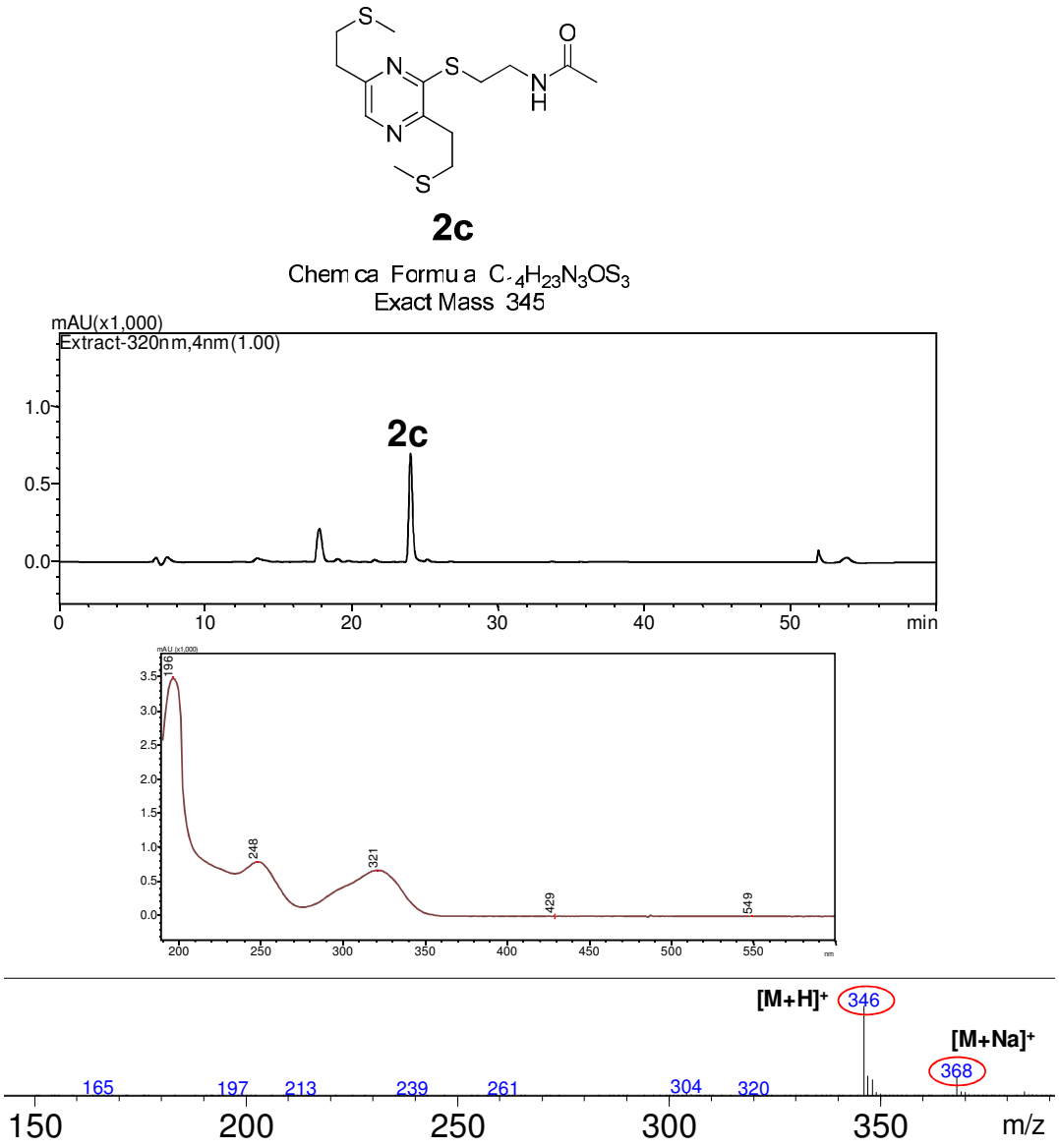

Figure S25. LC-MS and UV data for biosynthesized **2c**. **2c** is synthesized by NRPS325 with L-methionine in the presence of ATP, NAC and NADPH. From top to bottom: LC chromatogram (320nm), the UV absorption of **2c**, positive mass ionizations ($[M+H]^+$and $[M+Na]^+$) in the ESI-MS spectrum.

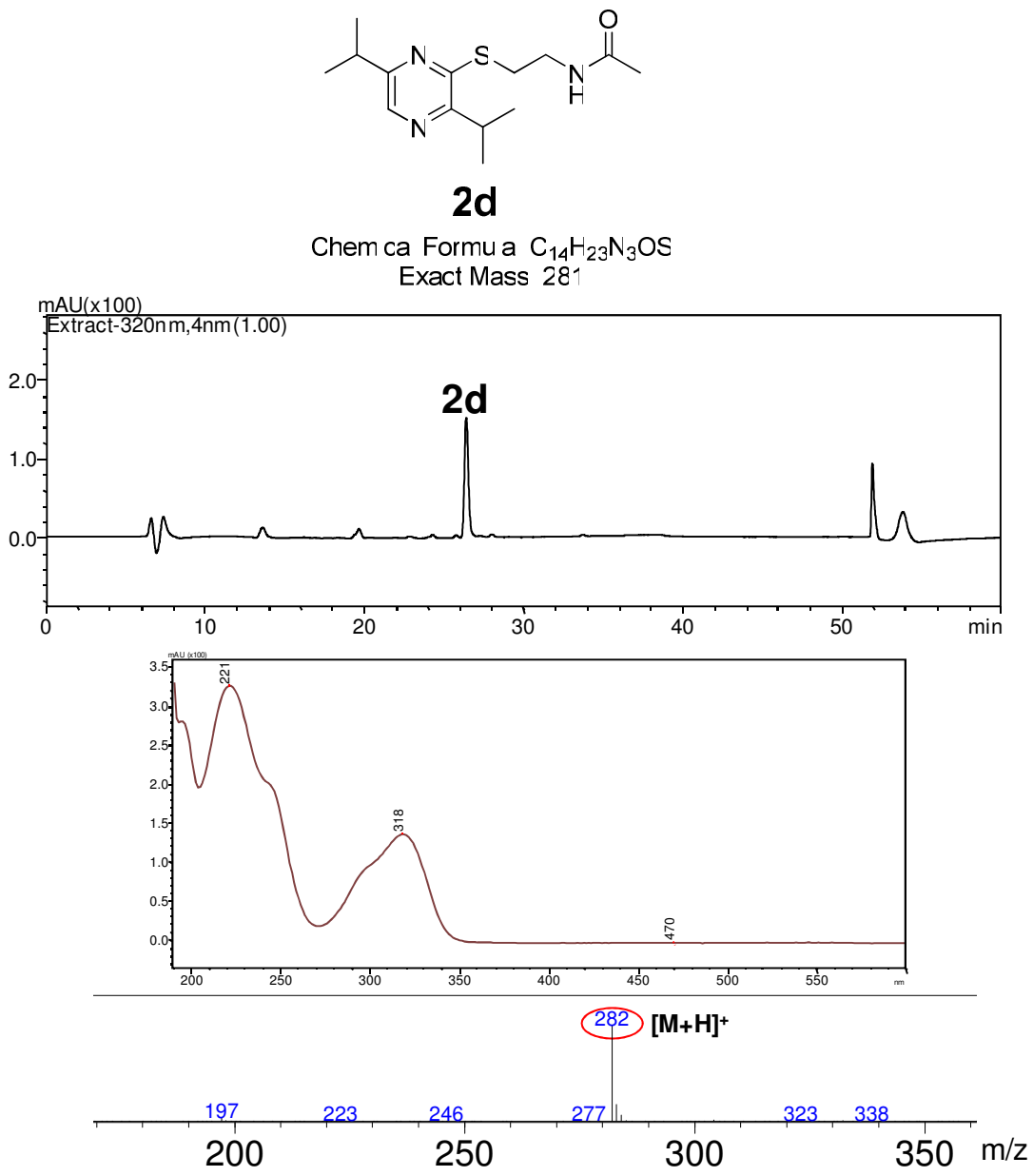

Figure S26. LC-MS and UV data for biosynthesized **2d**. **2d** is synthesized by NRPS325 with L-valine in the presence of ATP, NAC and NADPH. From top to bottom: LC chromatogram (320nm), the UV absorption of **2d**, positive mass ionizations ($[M+H]^+$and $[M+Na]^+$) in the ESI-MS spectrum.

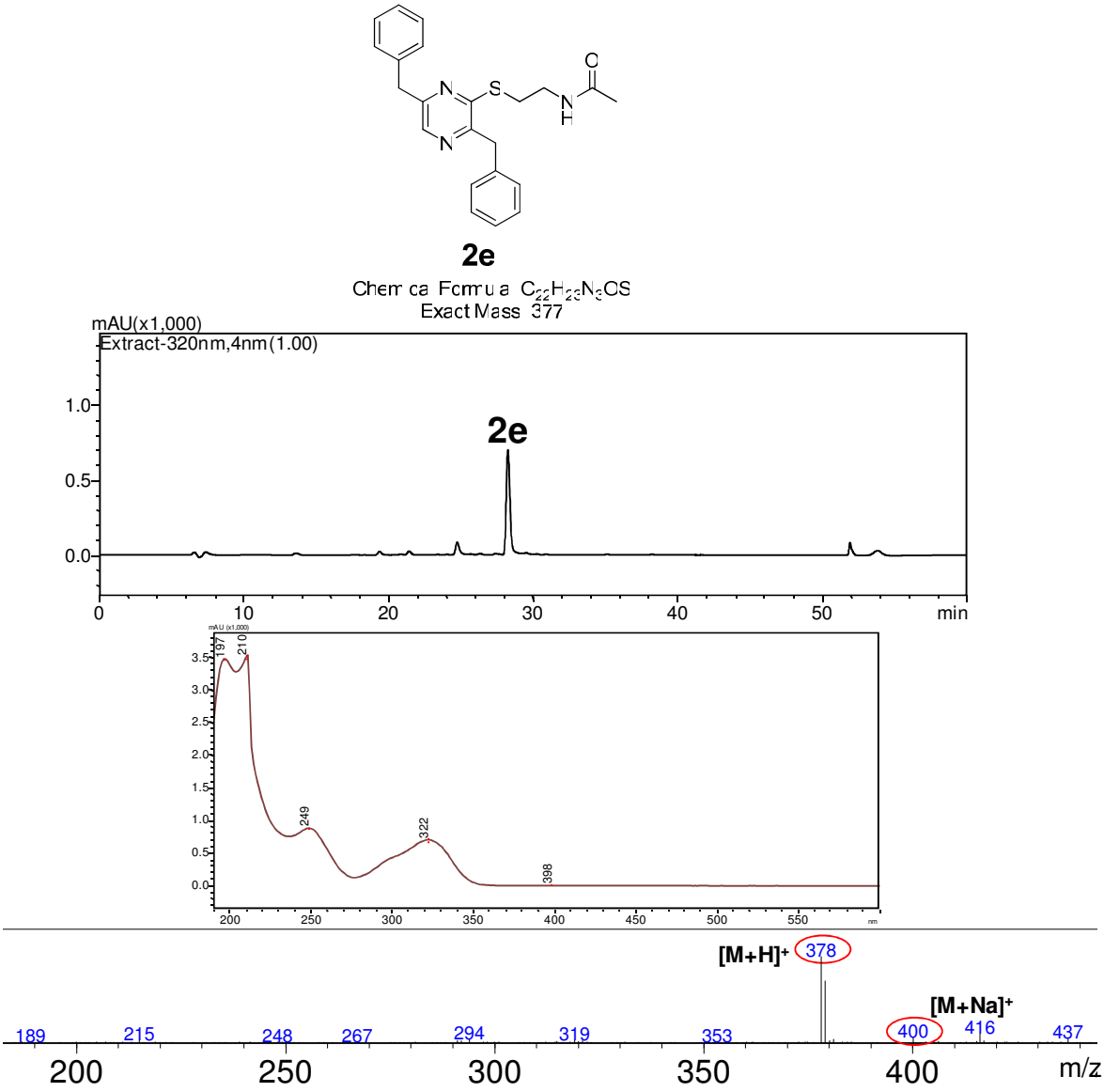

Figure S27. LC-MS and UV data for biosynthesized **2e**. **2e** is synthesized by NRPS325 with L-phenylalanine in the presence of ATP, NAC and NADPH. From top to bottom: LC chromatogram (320nm), the UV absorption of **2e**, positive mass ionizations ($[M+H]^+$and $[M+Na]^+$) in the ESI-MS spectrum.

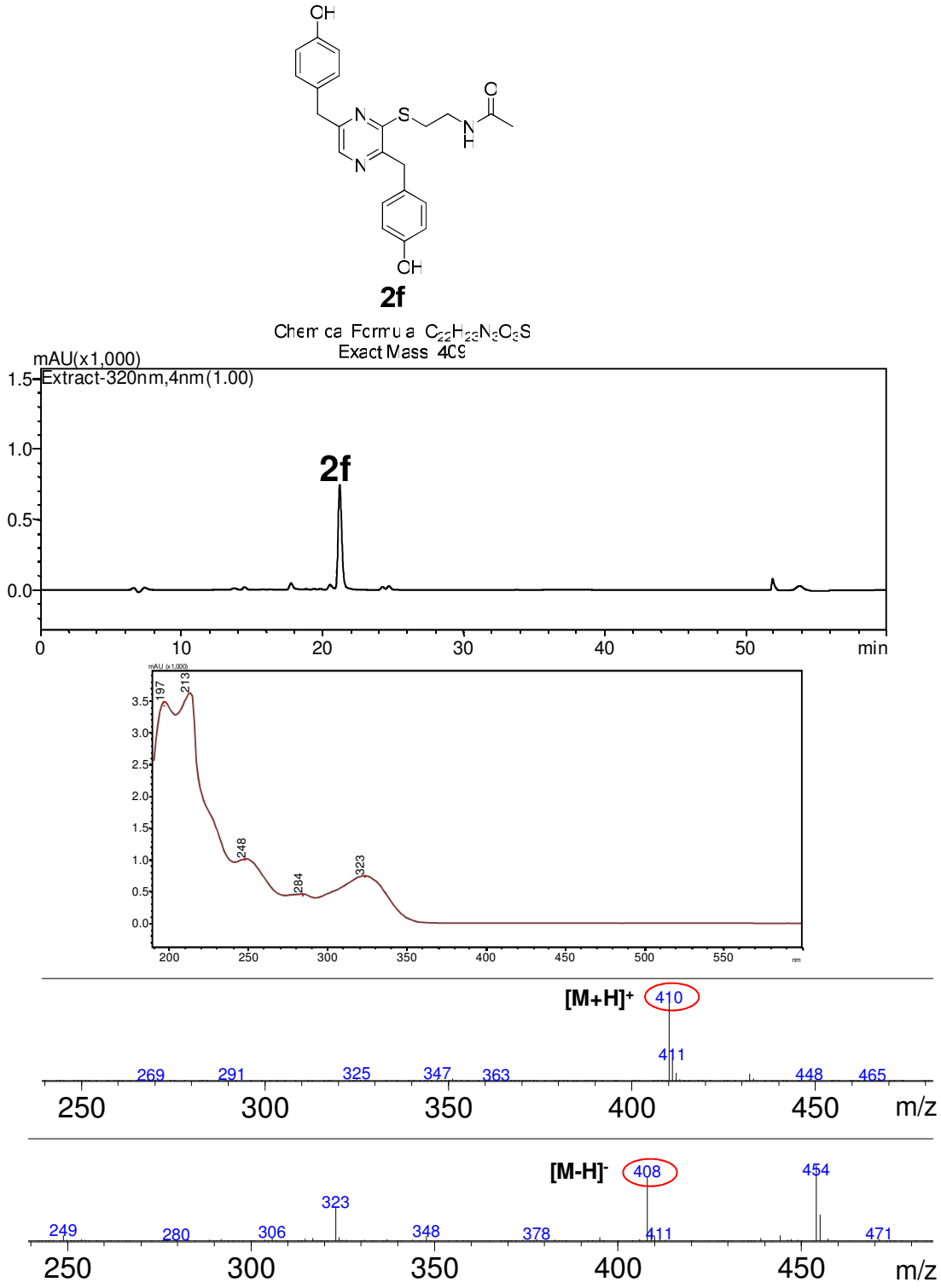

Figure S28. LC-MS and UV data for biosynthesized **2f**. **2f** is synthesized by NRPS325 with L-tyrosine in the presence of ATP, NAC and NADPH. From top to bottom: LC chromatogram (320nm), the UV absorption of **2f**, positive ($[M+H]^+$) and negative ($[M-H]^-$) ionizations in the ESI-MS spectra.

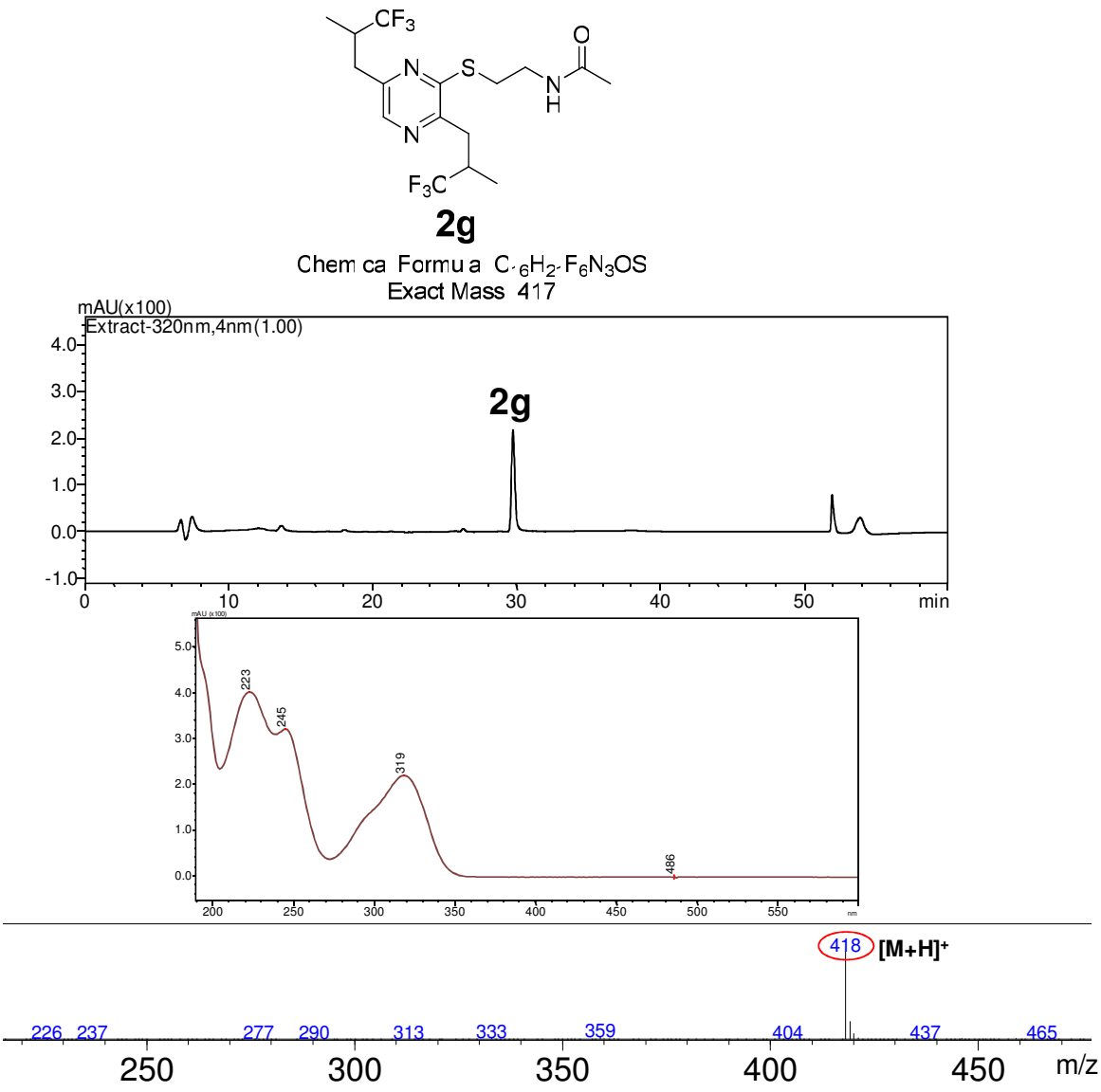

Figure S29. LC-MS and UV data for biosynthesized **2g**. **2g** is synthesized by NRPS325 with trifluoroleucine in the presence of ATP, NAC and NADPH. From top to bottom: LC chromatogram (320nm), the UV absorption of **2g**, positive ($[M+H]^+$) mass ionization in the ESI-MS spectrum.

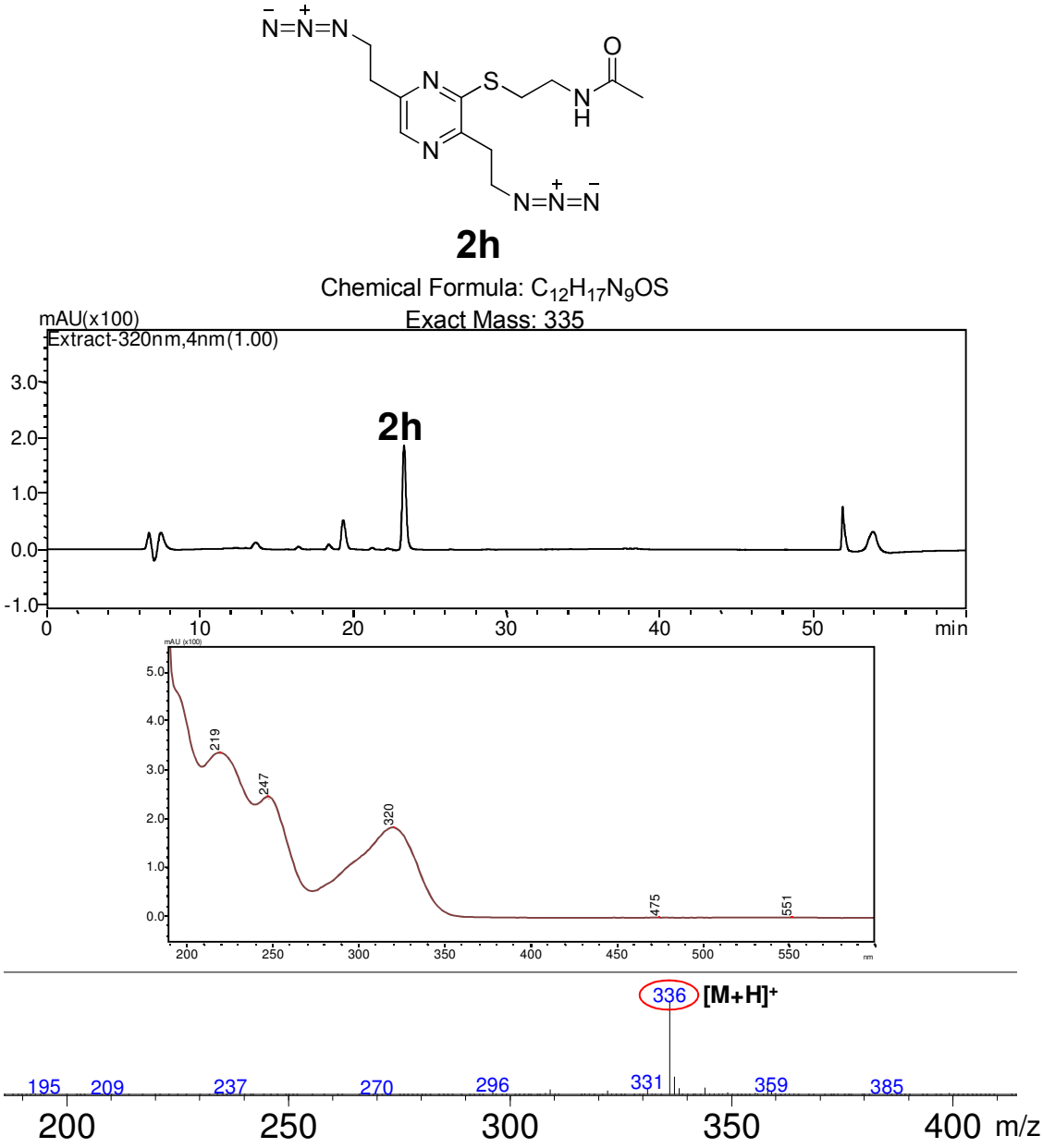

Figure S30. LC-MS and UV data for biosynthesized **2h**. **2h** is synthesized by NRPS325 with azidohomoalanine in the presence of ATP, NAC and NADPH. From top to bottom: LC chromatogram (320nm), the UV absorption of **2h**, positive ($[M+H]^+$) mass ionization in the ESI-MS spectrum.

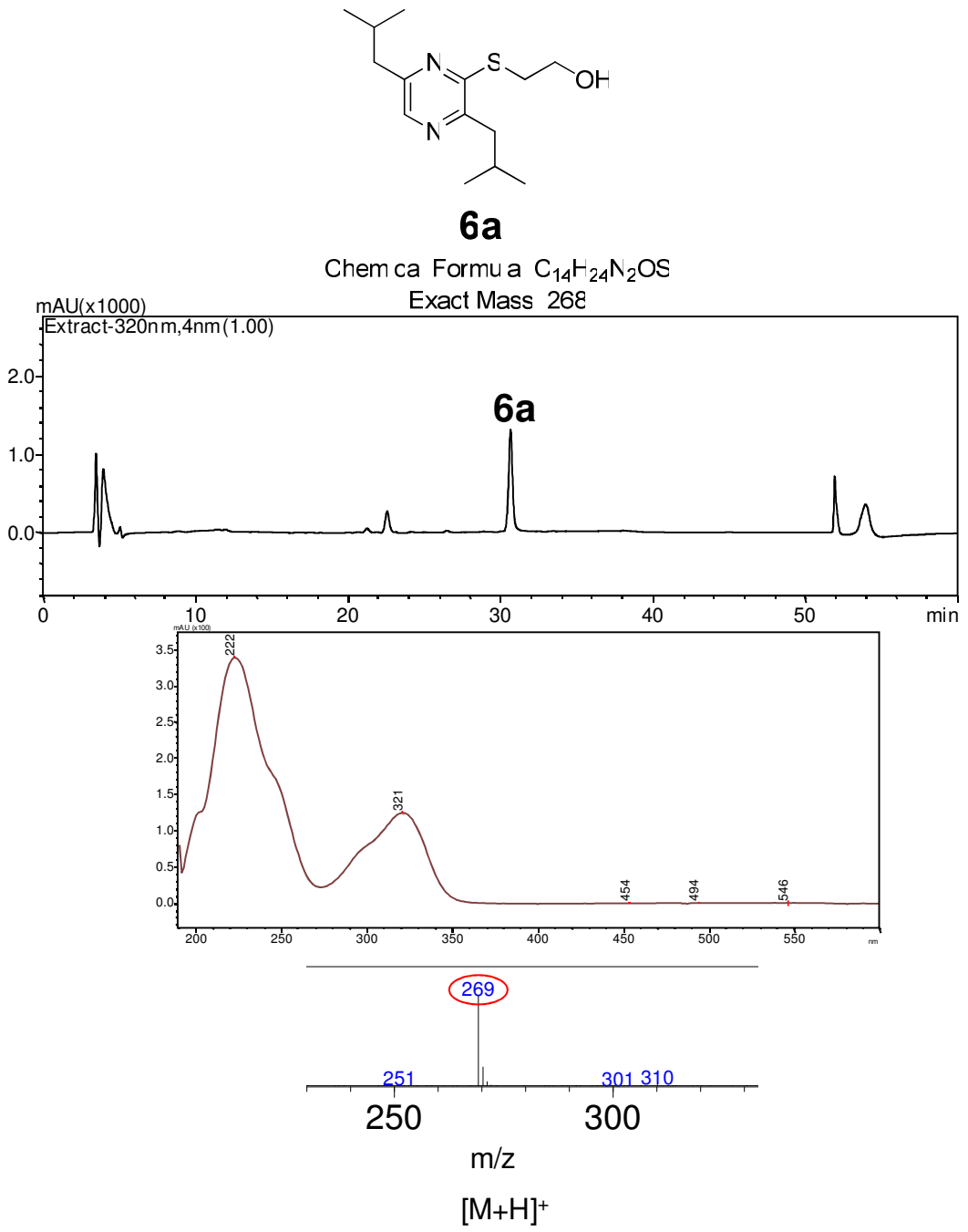

Figure S31. LC-MS and UV data for biosynthesized **6a**. **6a** is synthesized by NRPS325 with L-leucine in the presence of ATP, mercaptoethanol and NADPH. From top to bottom: LC chromatogram (320nm), the UV absorption of **6a**, positive ($[M+H]^+$) mass ionization in the ESI-MS spectrum.

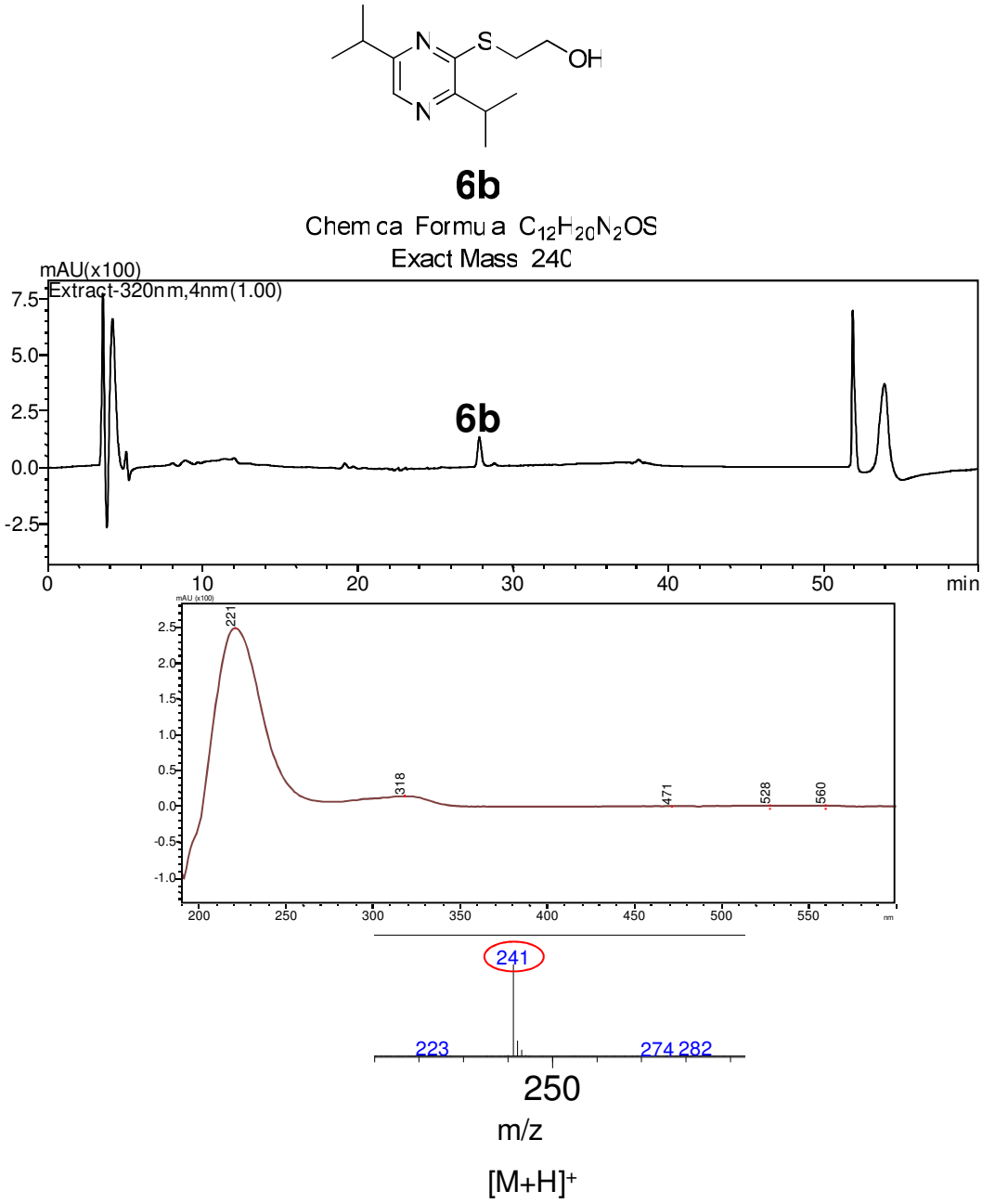

Figure S32. LC-MS and UV data for biosynthesized **6b**. **6b** is synthesized by NRPS325 with L-valine in the presence of ATP, mercaptoethanol and NADPH. From top to bottom: LC chromatogram (320nm), the UV absorption of **6b**, positive ($[M+H]^+$) mass ionization in the ESI-MS spectrum.

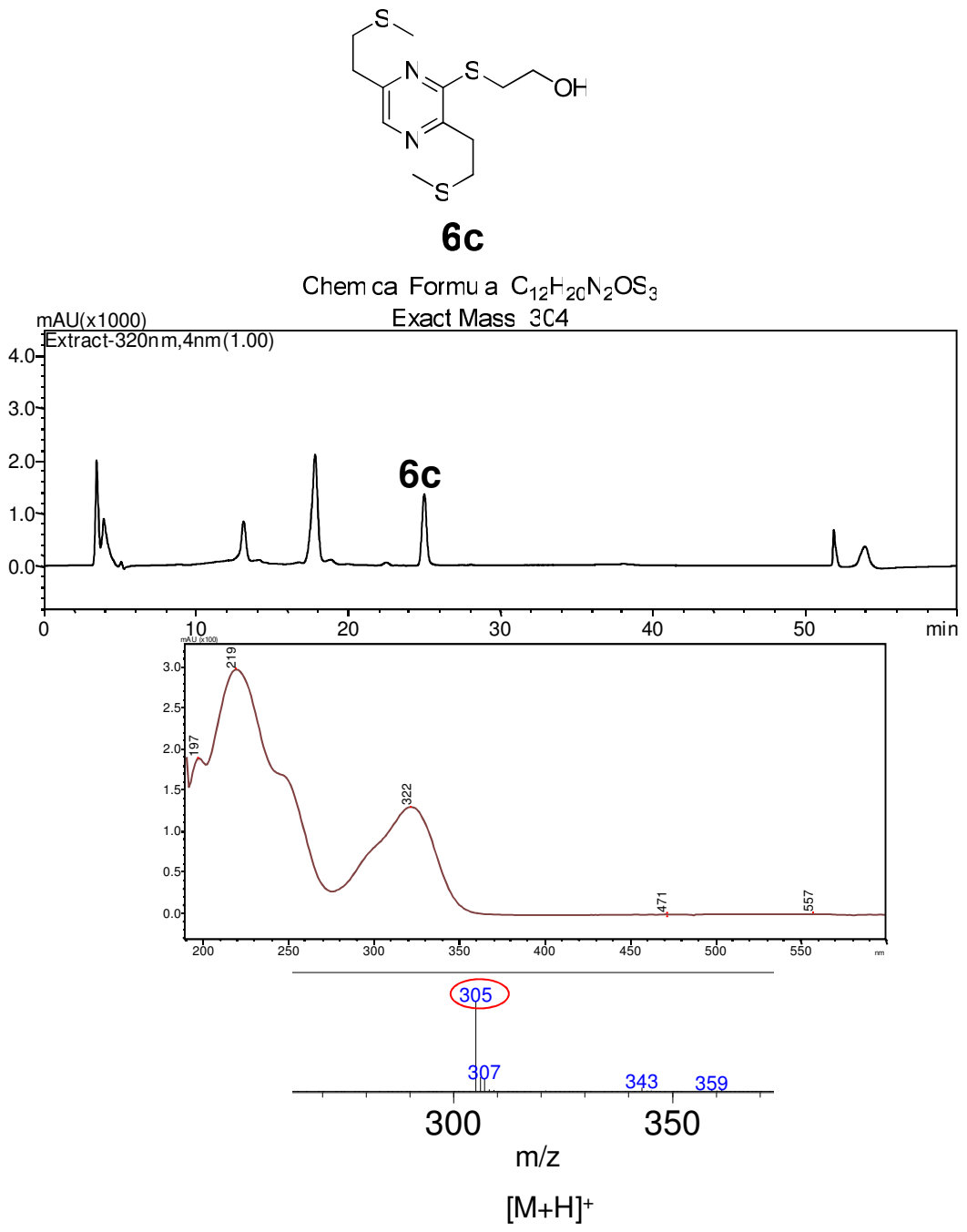

Figure S33. LC-MS and UV data for biosynthesized **6c**. **6c** is synthesized by NRPS325 with L-methionine in the presence of ATP, mercaptoethanol and NADPH. From top to bottom: LC chromatogram (320nm), the UV absorption of **6c**, positive ($[M+H]^+$) mass ionization in the ESI-MS spectrum.

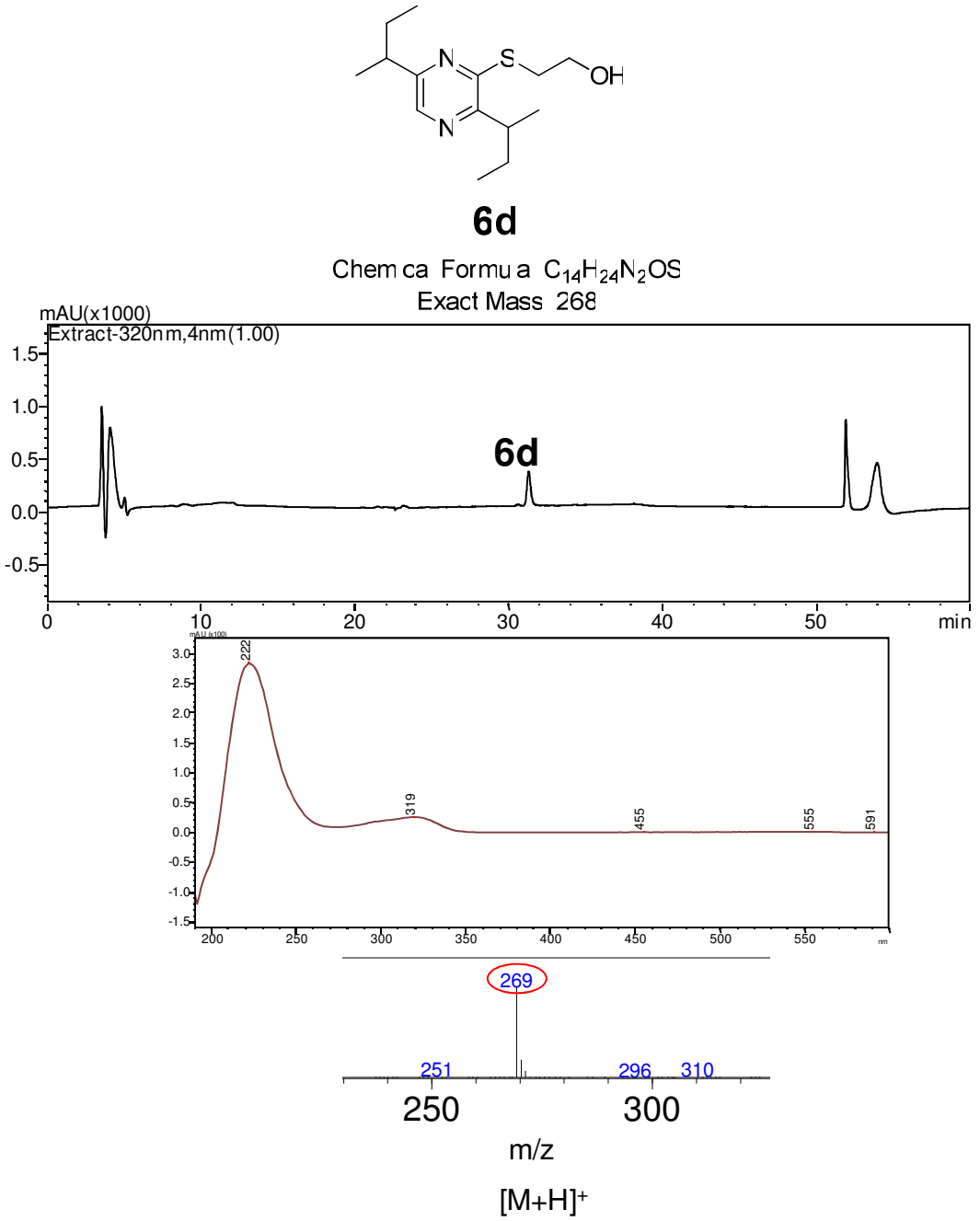

Figure S34. LC-MS and UV data for biosynthesized **6d**. **6d** is synthesized by NRPS325 with L-leucine in the presence of ATP, mercaptoethanol and NADPH. From top to bottom: LC chromatogram (320nm), the UV absorption of **6d**, positive ($[M+H]^+$) mass ionization in the ESI-MS spectrum.

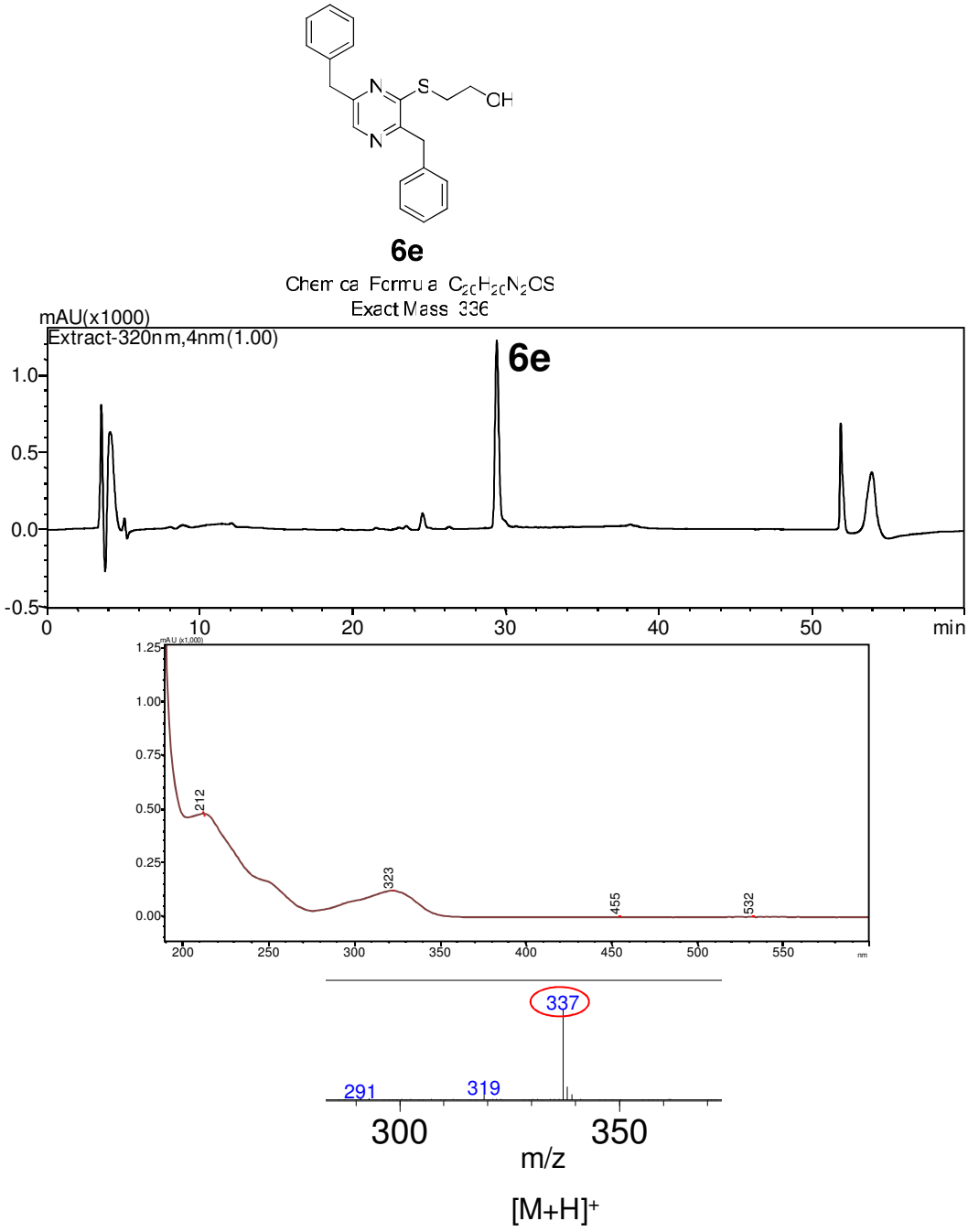

Figure S35. LC-MS and UV data for biosynthesized **6e**. **6e** is synthesized by NRPS325 with L-phenylalanine in the presence of ATP, mercaptoethanol and NADPH. From top to bottom: LC chromatogram (320nm), the UV absorption of **6e**, positive ($[M+H]^+$) mass ionization in the ESI-MS spectrum.

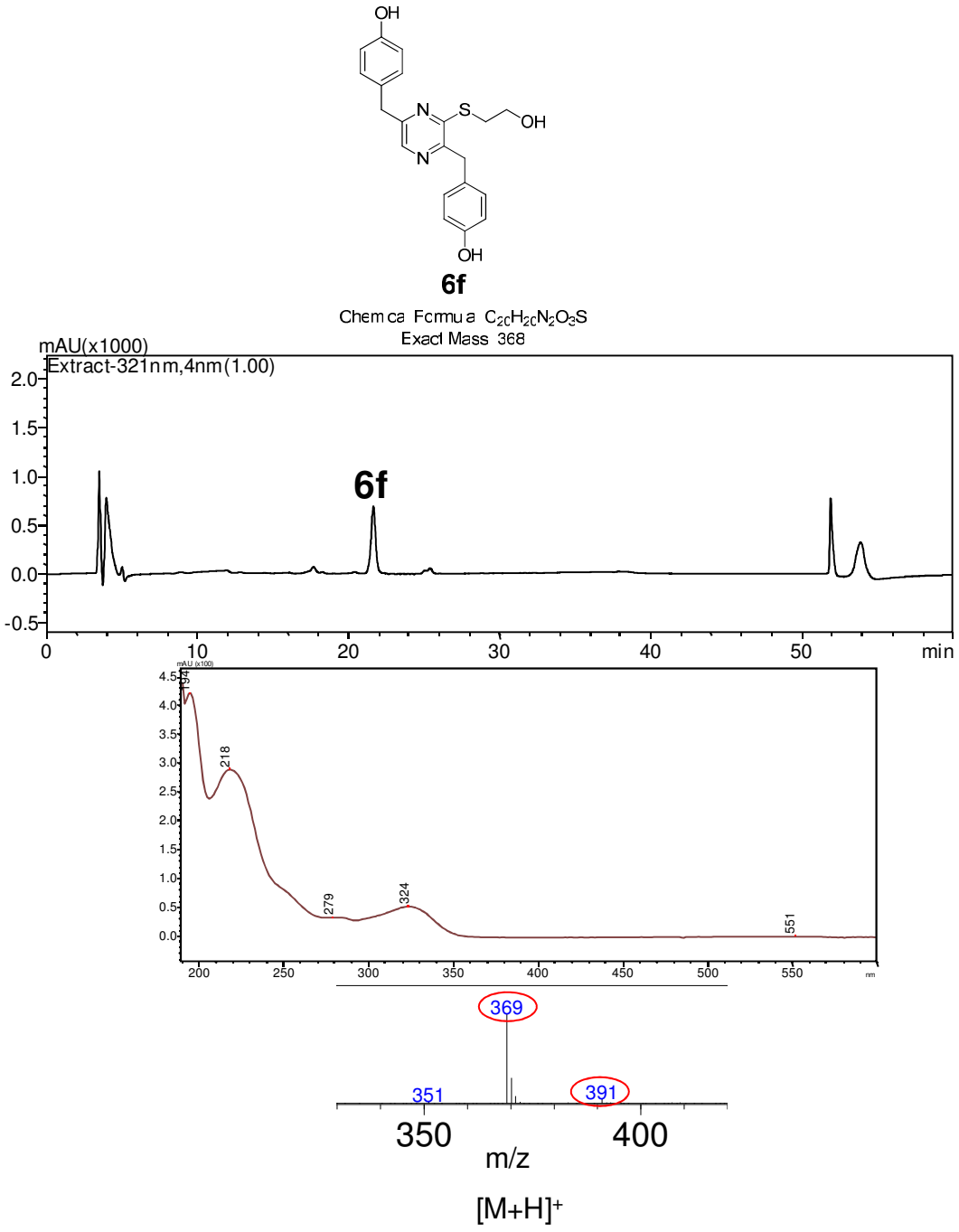

Figure S36. LC-MS and UV data for biosynthesized **6f**. **6f** is synthesized by NRPS325 with L-tyrosine in the presence of ATP, mercaptoethanol and NADPH. From top to bottom: LC chromatogram (320nm), the UV absorption of **6f**, positive ($[M+H]^+$) mass ionization in the ESI-MS spectrum.

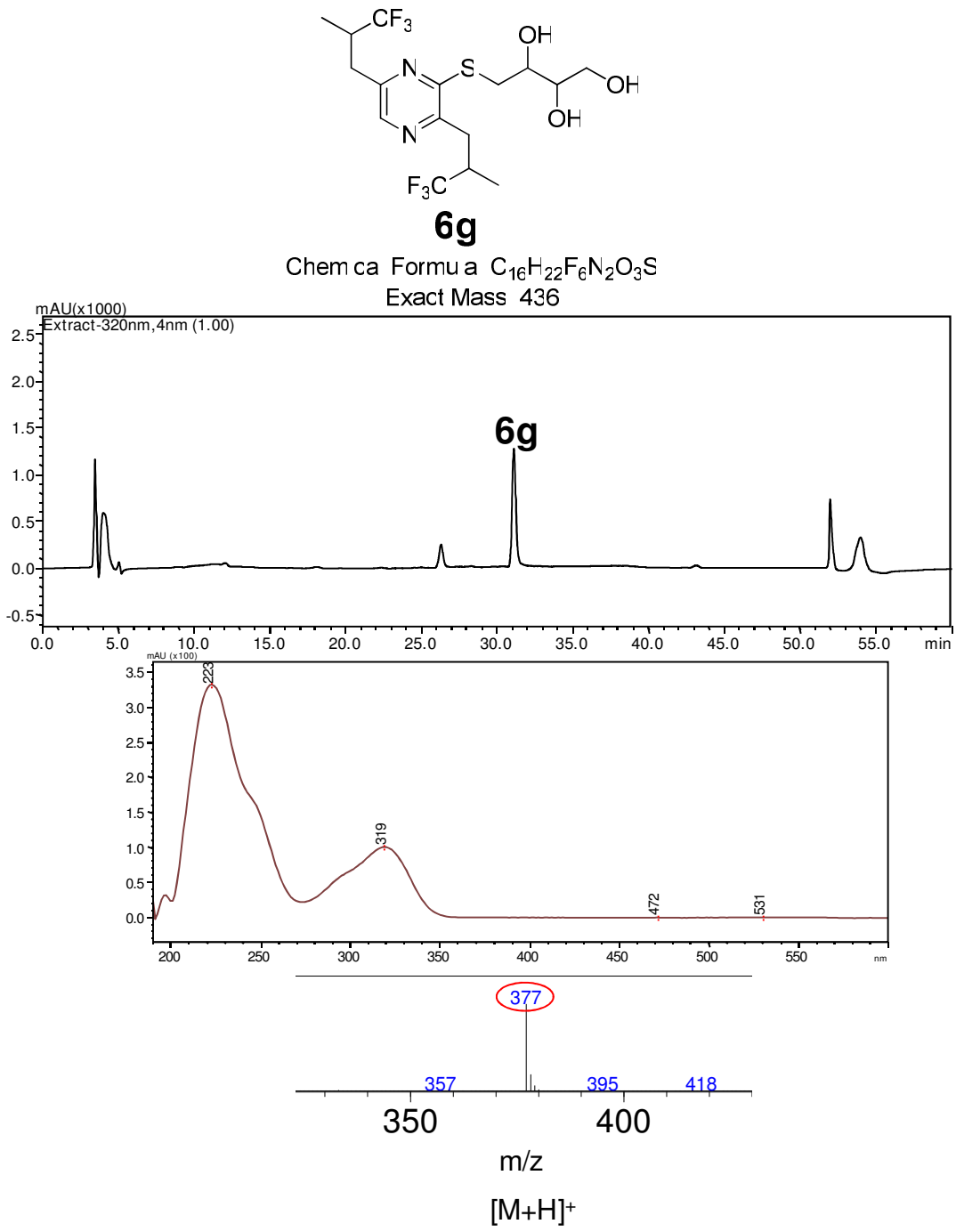

Figure S37. LC-MS and UV data for biosynthesized **6g**. **6g** is synthesized by NRPS325 with trifluoroleucine in the presence of ATP, mercaptoethanol and NADPH. From top to bottom: LC chromatogram (320nm), the UV absorption of **6g**, positive ($[M+H]^+$) mass ionization in the ESI-MS spectrum.

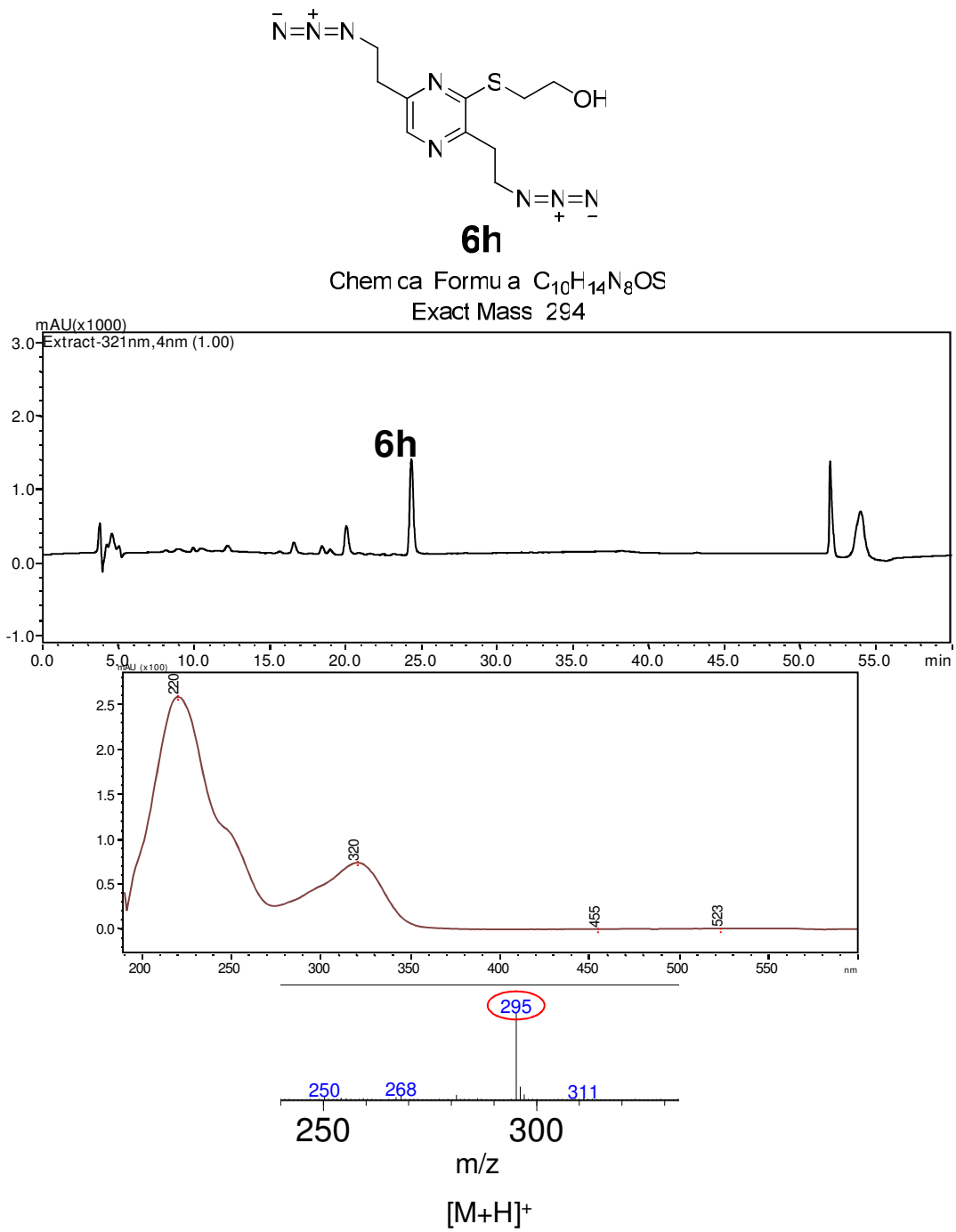

Figure S38. LC-MS and UV data for biosynthesized **6h**. **6h** is synthesized by NRPS325 with azidohomoalanine in the presence of ATP, mercaptoethanol and NADPH. From top to bottom: LC chromatogram (320nm), the UV absorption of **6h**, positive ($[M+H]^+$) mass ionization in the ESI-MS spectrum.

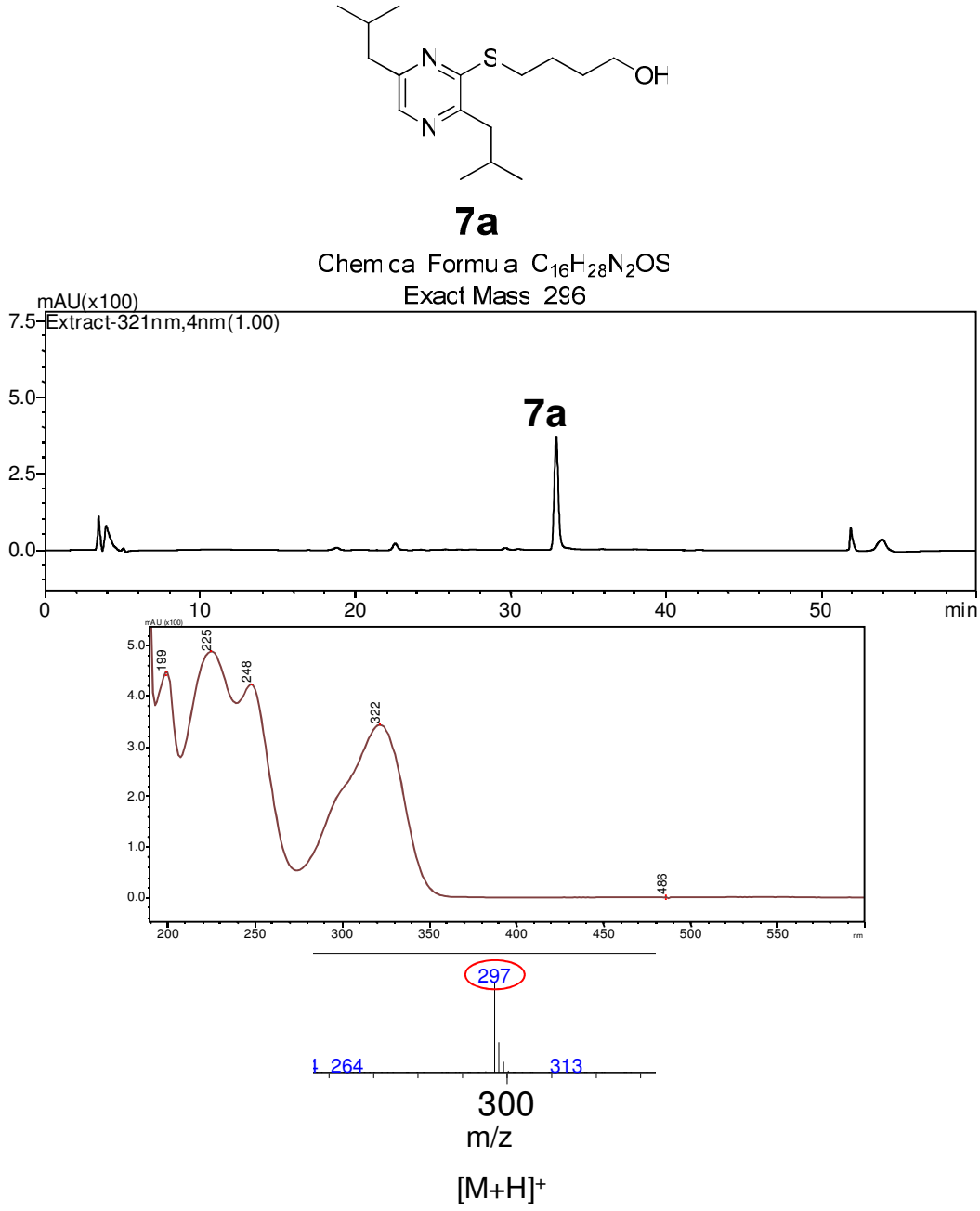

Figure S39. LC-MS and UV data for biosynthesized **7a**. **7a** is synthesized by NRPS325 with L-leucine in the presence of ATP, 4-mercapto-1-butanol and NADPH. From top to bottom: LC chromatogram (321nm), the UV absorption of **7a**, positive ($[M+H]^+$) mass ionization in the ESI-MS spectrum.

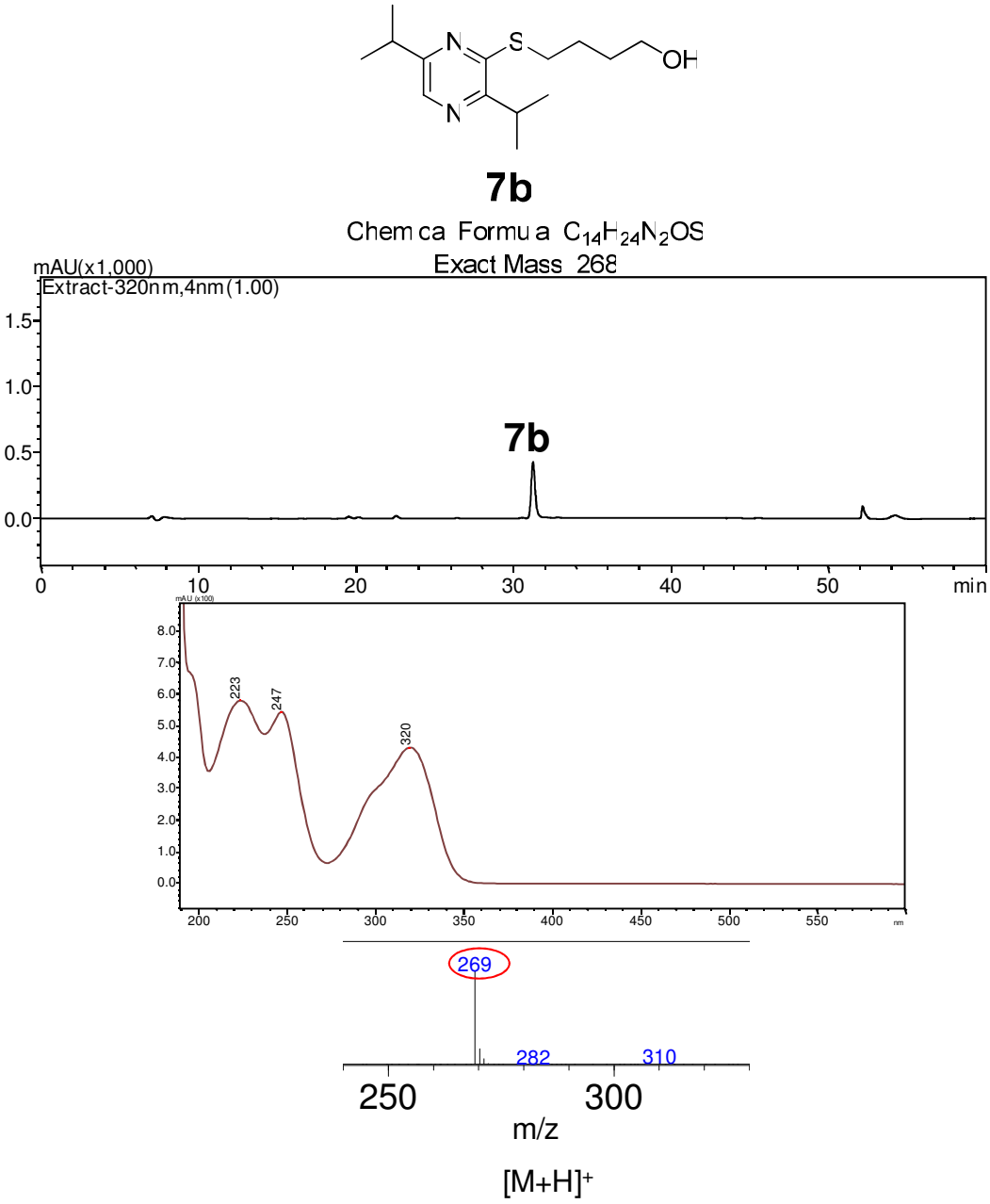

Figure S40. LC-MS and UV data for biosynthesized **7b**. **7b** is synthesized by NRPS325 with L-valine in the presence of ATP, 4-mercapto-1-butanol and NADPH. From top to bottom: LC chromatogram (320nm), the UV absorption of **7b**, positive ($[M+H]^+$) mass ionization in the ESI-MS spectrum.

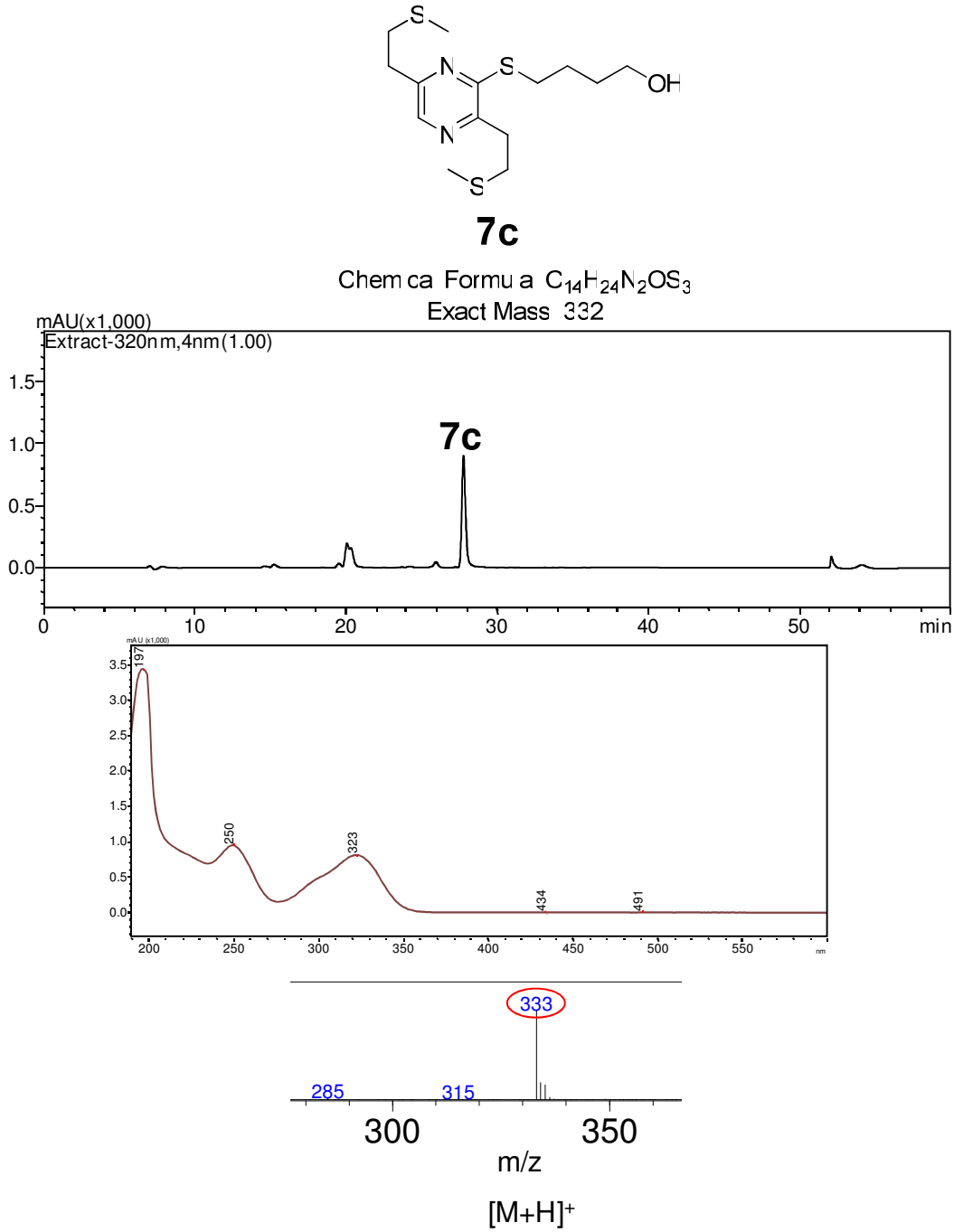

Figure S41. LC-MS and UV data for biosynthesized **7c**. **7c** is synthesized by NRPS325 with L-methionine in the presence of ATP, 4-mercapto-1-butanol and NADPH. From top to bottom: LC chromatogram (320nm), the UV absorption of **7c**, positive ($[M+H]^+$) and negative ($[M-H]^-$) mass ionizations in the ESI-MS spectra.

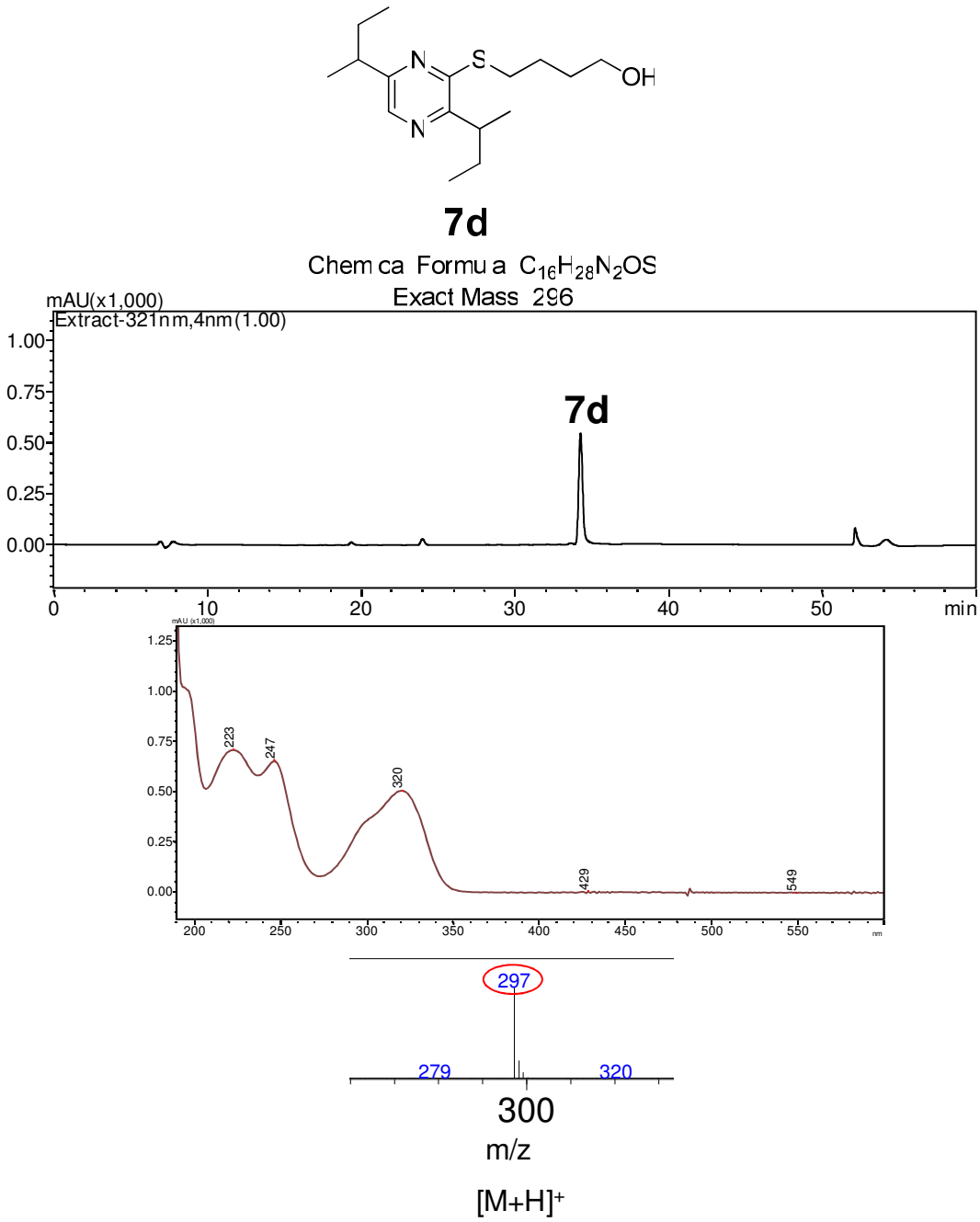

Figure S42. LC-MS and UV data for biosynthesized **7d**. **7d** is synthesized by NRPS325 with L-isoleucine in the presence of ATP, 4-mercapto-1-butanol and NADPH. From top to bottom: LC chromatogram (321nm), the UV absorption of **7d**, positive ($[M+H]^+$) mass ionization in the ESI-MS spectrum.

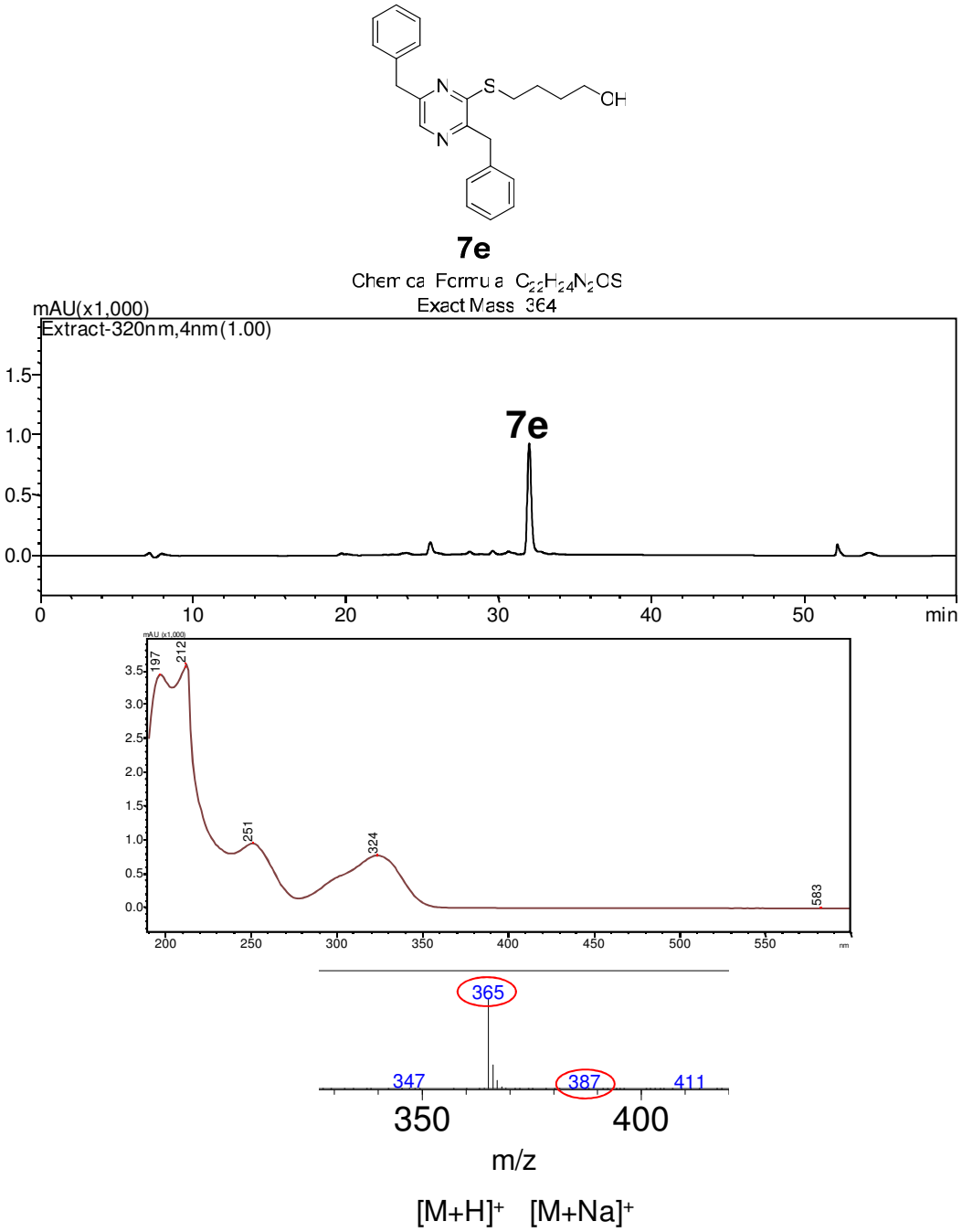

Figure S43. LC-MS and UV data for biosynthesized **7e**. **7e** is synthesized by NRPS325 with L-phenylalanine in the presence of ATP, 4-mercapto-1-butanol and NADPH. From top to bottom: LC chromatogram (320nm), the UV absorption of **7e**, positive ($[M+H]^+$) mass ionization in the ESI-MS spectrum.

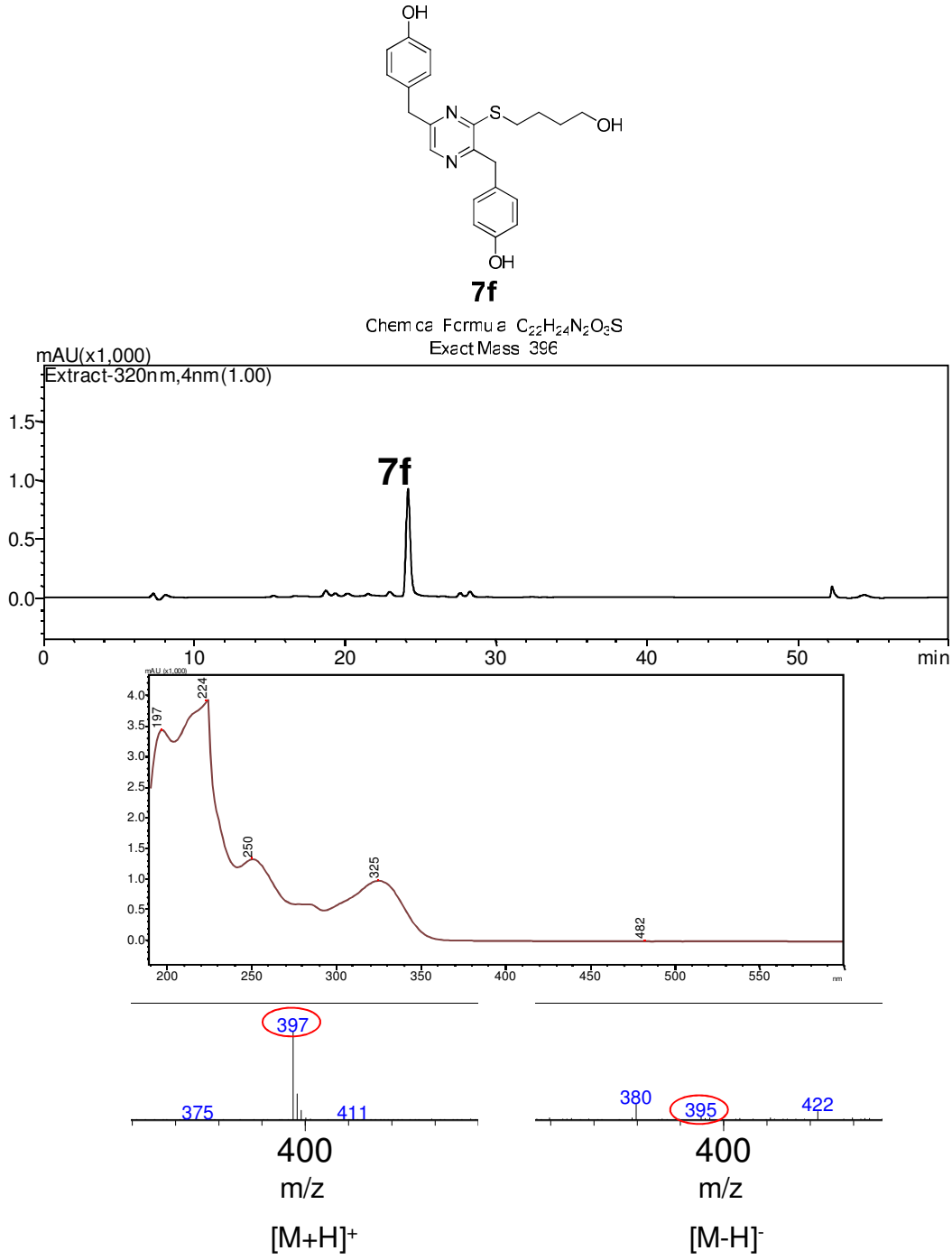

Figure S44. LC-MS and UV data for biosynthesized **7f**. **7f** is synthesized by NRPS325 with L-tyrosine in the presence of ATP, 4-mercapto-1-butanol and NADPH. From top to bottom: LC chromatogram (320nm), the UV absorption of **7f**, positive ($[M+H]^+$) mass ionization in the ESI-MS spectrum.

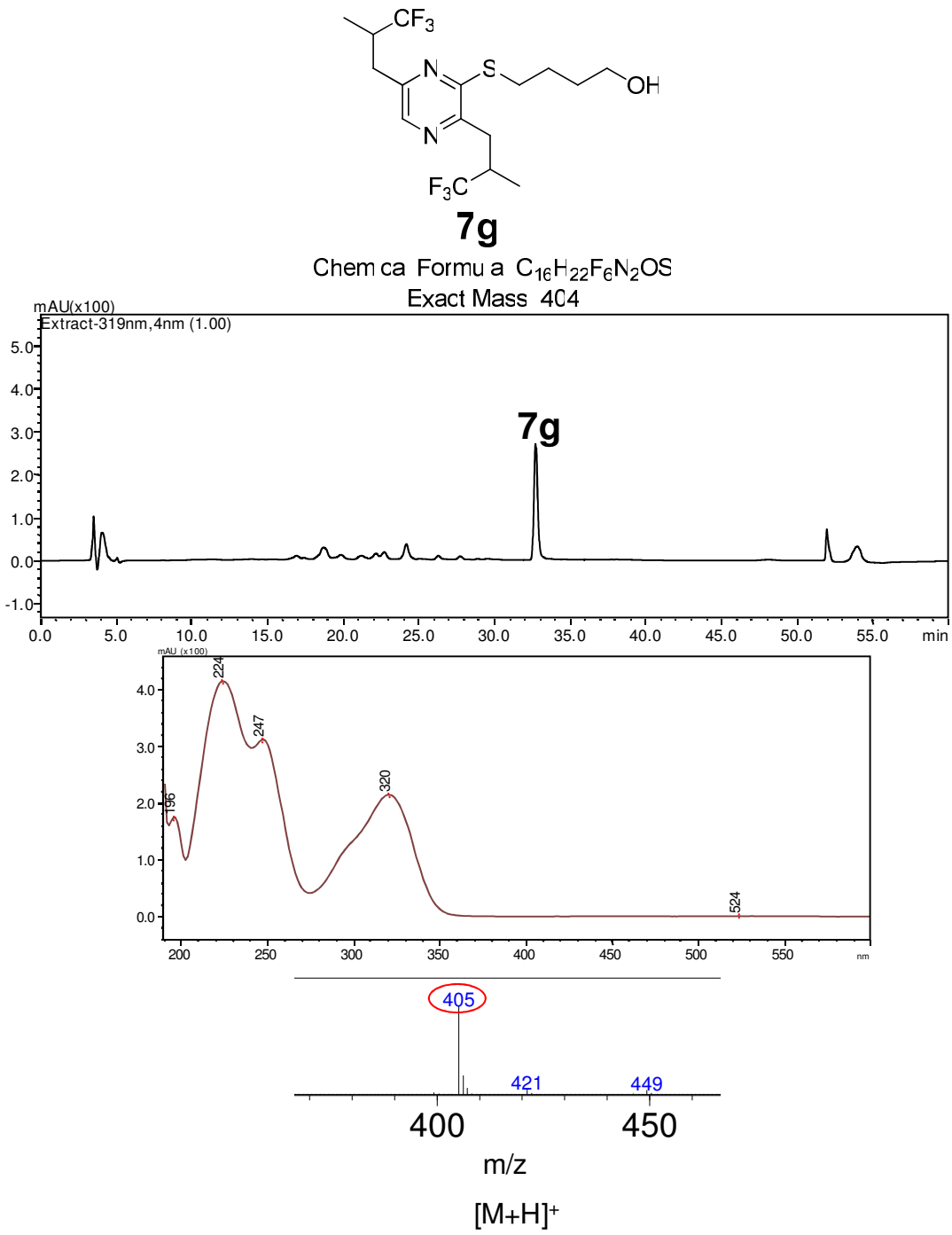

Figure S45. LC-MS and UV data for biosynthesized **7g**. **7g** is synthesized by NRPS325 with trifluoroleucine in the presence of ATP, 4-mercapto-1-butanol and NADPH. From top to bottom: LC chromatogram (319nm), the UV absorption of **7g**, positive ($[M+H]^+$) mass ionization in the ESI-MS spectrum.

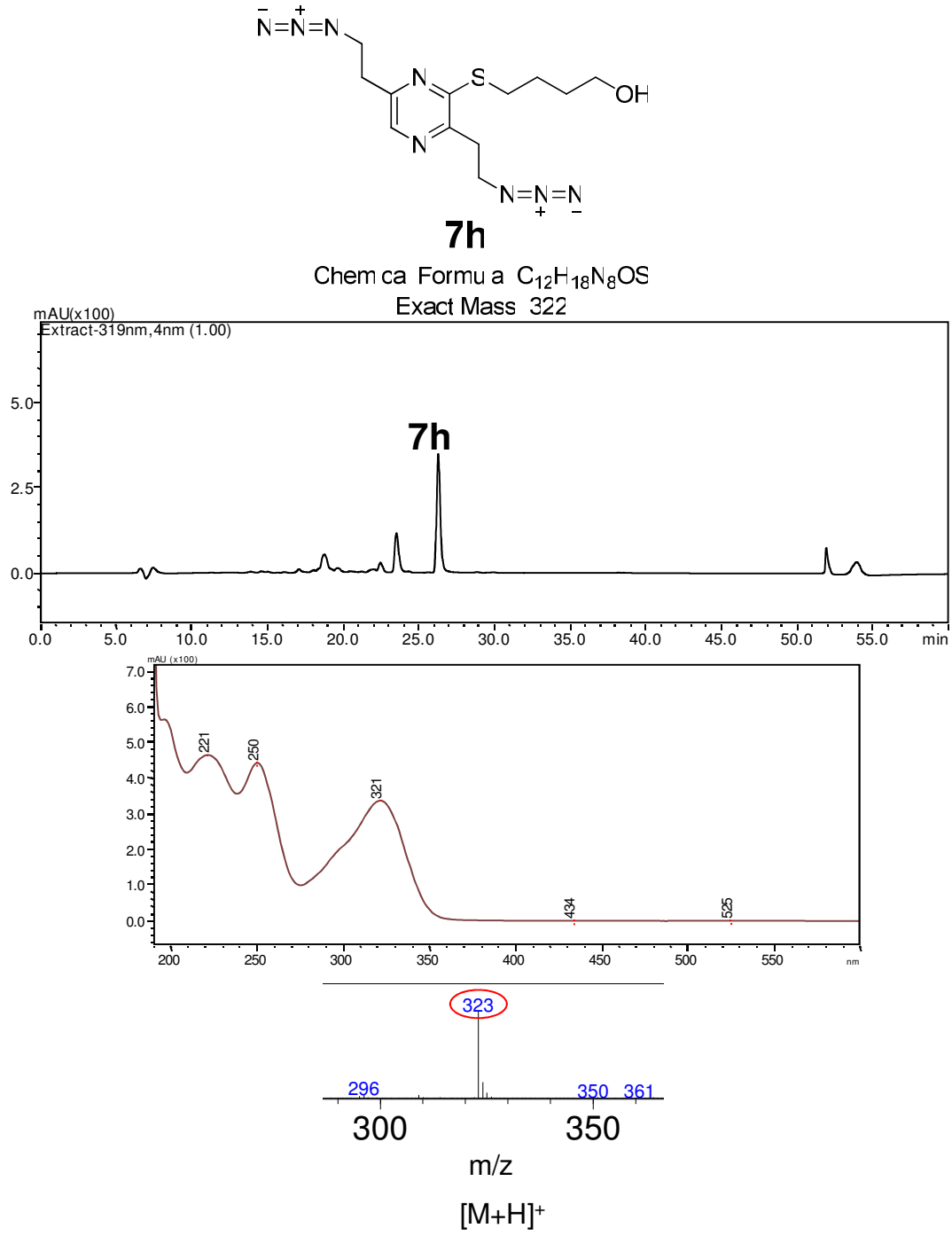

Figure S46. LC-MS and UV data for biosynthesized **7h**. **7h** is synthesized by NRPS325 with azidohomoalanine in the presence of ATP, 4-mercapto-1-butanol and NADPH. From top to bottom: LC chromatogram (319nm), the UV absorption of **7h**, positive ($[M+H]^+$) mass ionization in the ESI-MS spectrum.

3. REFERENCE

(1) O'Brien, W. E. *Anal. Biochem.* **1976**, *76*, 423.
(2) Ehmann, D. E.; Trauger, J. W.; Stachelhaus, T.; Walsh, C. T. *Chem. Biol.* **2000**, *7*, 765.
(3) Muller, T.; Bezegh, A.; Dancso, J. *Mag. Kem. Foly.* **1981**, *87*, 429.
(4) Dromey, R. G.; Foyster, G. T. *Anal. Chem.* **1980**, *52*, 394.